AD-A098 109 NAVAL WEAPONS CENTER CHINA LAKE CA F/G 16/4
EVALUATION OF STATISTICAL FRACTURE CRITERIA FOR MAGNESIUM FLUOR--ETC(U)
DEC 80 M D HERR, W R COMPTON
UNCLASSIFIED NWC-TP-6226 SBIE-AD-E900 078 NL

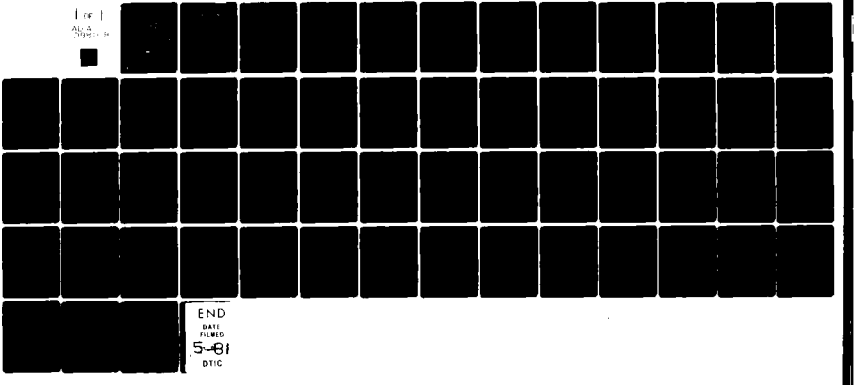

END
DATE FILMED
5-81
DTIC

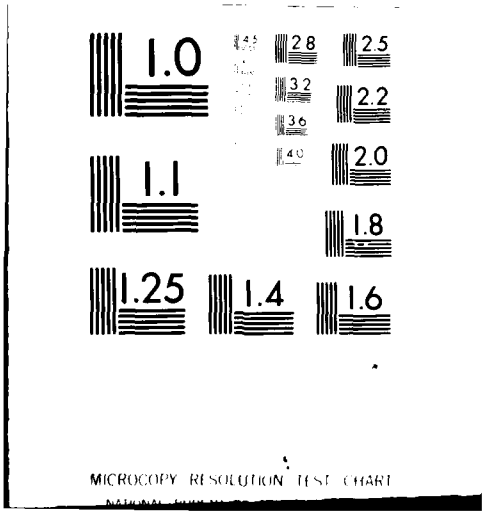
1.0
1.1
1.25
1.4
1.6
1.8
2.0
2.2
2.5
2.8
3.2
3.6
4.0
MICROCOPY RESOLUTION TEST CHART

NWC TP 6226

EVALUATION OF STATISTICAL FRACTURE CRITERIA FOR MAGNESIUM FLUORIDE SEEKER DOMES

by
M. D. Herr
and
W. R. Compton
Ordnance Systems Department

DECEMBER 1980

NAVAL WEAPONS CENTER
CHINA LAKE, CALIFORNIA 93555

Naval Weapons Center

AN ACTIVITY OF THE NAVAL MATERIAL COMMAND

FOREWORD

This report documents an evaluation of statistical fracture theories as applied to aerodynamic heating of full-scale seeker domes. Dome fracture data obtained from aerodynamic heating tests of magnesium fluoride domes were used to evaluate these fracture theories. The work was performed during fiscal years 1978 and 1979.

This effort was supported by the Naval Air Systems Command (NAVAIR) and executed by the Naval Weapons Center (NWC) under the Strike Warfare Weaponry Technology Block Program under AirTask A03W-03P2/008B/8F32-300-000 and 9F32-300-000. This AirTask provides for continued exploratory development in air superiority and air-to-surface mission areas. Mr. William Volz (AIR-320C) was the cognizant NAVAIR Technology Administrator.

Mr. C. F. Markarian has reviewed this report for technical accuracy.

Approved by
C. L. SCHANIEL, *Head*
Ordnance Systems Department
1 December 1980

Under authority of
W. B. HAFF
Capt., U.S. Navy
Commander

Released for publication by
R. M. HILLYER
Technical Director

NWC Technical Publication 6226

Published by . . . . . Technical Information Department
Collation . . . . . Cover, 27 leaves
First printing . . . . . 120 unnumbered copies

REPORT DOCUMENTATION PAGE	READ INSTRUCTIONS BEFORE COMPLETING FORM
NWC TP 6226 AD-A098109	
4. TITLE (and Subtitle) EVALUATION OF STATISTICAL FRACTURE CRITERIA FOR MAGNESIUM FLUORIDE SEEKER DOMES	5. TYPE OF REPORT & PERIOD COVERED 1978-1979 6. PERFORMING ORG. REPORT NUMBER
7. AUTHOR(s) M. D. Herr and W. R. Compton	8. CONTRACT OR GRANT NUMBER(s) AirTask A03W-03P2/008B/ 8F32-300-000 9F32-300-000
9. PERFORMING ORGANIZATION NAME AND ADDRESS Naval Weapons Center China Lake, CA 93555	10. PROGRAM ELEMENT, PROJECT, TASK AREA & WORK UNIT NUMBERS
11. CONTROLLING OFFICE NAME AND ADDRESS	12. REPORT DATE December 1980 13. NUMBER OF PAGES 52
14. MONITORING AGENCY NAME & ADDRESS(if different from Controlling Office)	15. SECURITY CLASS. (of this report) UNCLASSIFIED 15a. DECLASSIFICATION/DOWNGRADING SCHEDULE

16. DISTRIBUTION STATEMENT (of this Report)

Approved for public release: distribution unlimited.

17. DISTRIBUTION STATEMENT (of the abstract entered in Block 20, if different from Report)

18. SUPPLEMENTARY NOTES

19. KEY WORDS (Continue on reverse side if necessary and identify by block number)

Aerodynamics
Missile Structures
Radomes

20. ABSTRACT (Continue on reverse side if necessary and identify by block number)

See reverse side of this form.

DD FORM 1 JAN 73 1473 EDITION OF 1 NOV 65 IS OBSOLETE
S/N 0102 LF 014 6601

(U) *Evaluation of Statistical Fracture Criteria for Magnesium Fluoride Seeker Domes*, by M. D. Herr and W. R. Compton. China Lake, Calif., Naval Weapons Center, December 1980, 52 pp. (NWC TP 6226, publication UNCLASSIFIED.)

(U) Four statistical fracture theories are applied to the problem of infrared dome fracture in an aerodynamic heating environment. Theoretical fracture predictions are compared with time-to-fracture data obtained for full-scale magnesium fluoride domes in an aerodynamic heating environment. The surface-distributed flaw theory of Batdorf proves to yield the most accurate predictions of the probability of dome fracture.

CONTENTS

ACKNOWLEDGMENT

The authors wish to express their gratitude for the efforts of L. D. Sawyer (NWC Materials Engineering Branch) Code 3624 in the design and fabrication of portions of the test hardware utilized in this investigation. The authors also wish to acknowledge the innovative efforts of L. M. Horgan of the T-Range facility (NWC Test Branch).

INTRODUCTION

The launch envelopes of heat-seeking missiles used on current combat aircraft are frequently restricted by the thermostructural limits of the infrared (IR) dome used in the seeker system. These limits are derived from the predicted fracture of the ceramic materials used in IR dome construction. In general, ceramics are brittle materials that exhibit a wide range of fracture strengths under apparently identical loading conditions. Consequently, unrealistically severe missile launch envelope restrictions are imposed on the aircraft in order to compensate for the uncertainties in the dome fracture strength.

The results of a previous investigation[1] gave indications that better definition of such launch envelope restrictions could be achieved through the use of the statistical fracture theories of Weibull[2,3] and Batdorf.[4,5] The limited amount of IR dome fracture data extant at the time of this previous investigation prevented a comprehensive evaluation of these fracture theories. In addition, the mathematical details required to utilize material fracture statistics from a variety of fracture strength test methods were not yet developed for the Batdorf theory. The current investigation extends the usefulness of the Batdorf theory by developing these mathematical details for three commonly employed strength test methods.

---

[1] W. R. Compton. *Application of Statistical Fracture Criteria to the Problem of Predicting Infrared Dome Thermal Shock Failures.* China Lake, Calif., NWC, January 1978. (NWC TP 6010, publication UNCLASSIFIED.)

[2] W. Weibull. "Statistical Theory of Strength of Materials," *Ing. Vetenskaps Akad. Handl.*, No. 151, 45 pp (1939); *Ceram. Abstr.*, 19[3] 78 (1949)

[3] W. Weibull. "Statistical Distribution Function of Wide Applicability," *J. Appl. Mech.*, 18[3] 293 (September 1971)

[4] The Aerospace Corporation. *Fracture Statistics of Brittle Materials with Intergranular Cracks*, by S. B. Batdorf. El Segundo, Calif., 10 October 1974. (SAMSO-TR-74-210, publication UNCLASSIFIED.)

[5] ———. *Fracture Statistics of Isotropic Brittle Materials with Surface Flaws*, by S. B. Batdorf. El Segundo, Calif., 3 December 1973. (SAMSO-TR-73-378, publication UNCLASSIFIED.)

Fracture statistics for IR dome materials are usually determined from flexural tests of small laboratory material specimens. Such material specimens frequently do not have the same internal grain structure or external surface preparation that exists for an IR dome. Consequently, any difference in the method of fabrication between the small material specimens and an IR dome may yield erroneous fracture statistics for the dome. Two sets of fracture statistics for the material magnesium fluoride (MgF_2) were used in this investigation in order to explore this problem area. One set of fracture statistics was obtained from four-point bending tests[6] of specimens with surface scratches less than $6(10)^{-4}$ inch deep (15 μm) and another was obtained from concentric ring bending tests[7] of specimens with surface scratches less than $4(10)^{-5}$ inch deep (1 μm). Both sets of material test specimens were fabricated from MgF_2 plate stock.

The objective of the present investigation was to obtain a comprehensive evaluation of the aforementioned fracture theories by direct comparisons with full-scale IR dome fracture statistics. The fracture statistics for IR domes were obtained by subjecting thirty MgF_2 domes to the same simulated free-flight thermal environment of the NWC T-Range hot gas facility. The statistical fracture theories were evaluated by comparing the predicted and observed probability of dome fracture as a function of time after the simulated missile launch.

DOME FRACTURE TESTS

Fracture data for IR domes were obtained at the NWC T-Range hot gas facility by subjecting 30 MgF_2 domes (Figure 1) to a thermal environment simulating the free-flight profile shown in Figure 2. The T-Range facility utilizes an axial flow propane burner in a blowdown wind tunnel to produce free-flight aerodynamic heating levels. The MgF_2 domes were mounted in the free-jet issuing from a convergent-divergent nozzle as shown in Figure 3. The free-flight thermal environment was simulated by varying the total pressure and temperature histories in the T-Range facility in such a way as to match the total conditions on the dome during free-flight (Table 1). The range of total pressure and temperature profiles actually observed during the test series is shown in Figures 4 and 5.

---

[6] Naval Weapons Center. *Report of Modulus of Rupture Tests on Magnesium Fluoride IR Dome Material*, by R. L. Smith. China Lake, Calif., NWC, 8 August 1972. (Reg. Memo 4062-010-73, UNCLASSIFIED.)

[7] ———. Unpublished test data for fracture strength of magnesium fluoride discs subjected to concentric ring loading, by R. J. Schiltz and G. A. Hayes. China Lake, Calif., NWC, 1975.

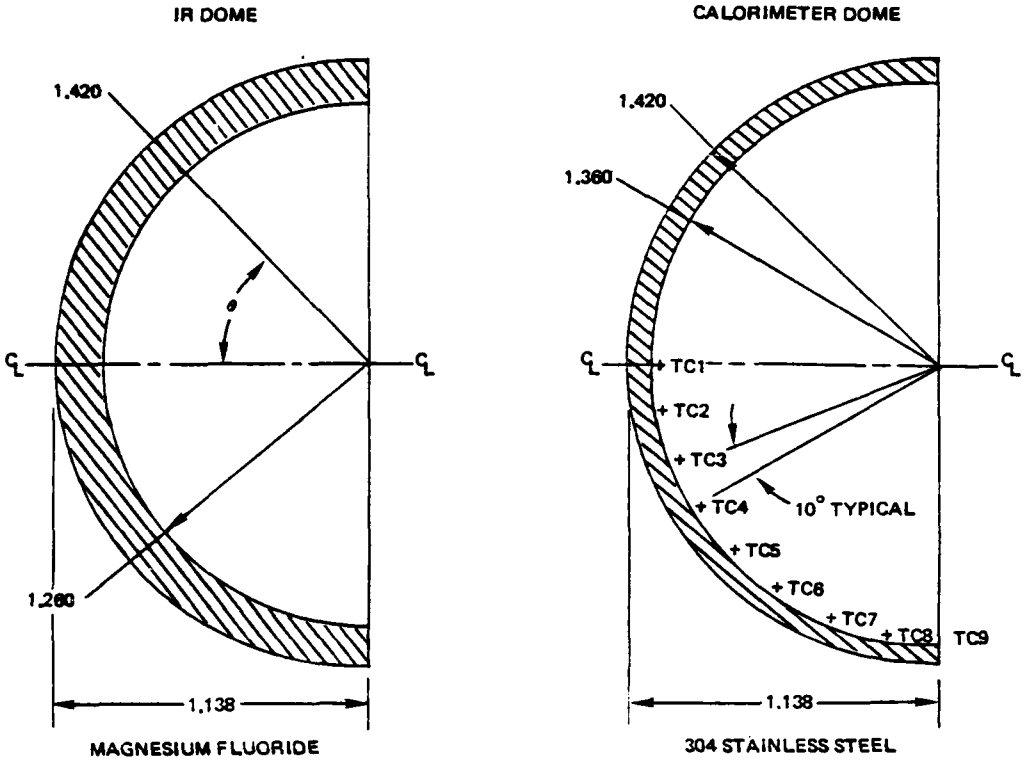

FIGURE 1. Magnesium Fluoride Dome Geometry.

The variation of the aerodynamic heat transfer coefficient with time and dome streamwise position was determined from the thermal response of a calorimeter dome constructed from 0.060 inch thick 304 stainless steel (see footnote 1). The heat transfer coefficient variation with time and dome streamwise position is shown in Figures 6 and 7. The heat transfer levels obtained in the free jet were found to be more severe than those encountered during free flight. This was due to the high turbulence levels inherent in the T-Range facility. The stagnation point heat transfer coefficient was roughly 40% higher than expected during a missile free flight. In addition, boundary layer transition occurred much closer to the dome stagnation point than would be expected during free flight.

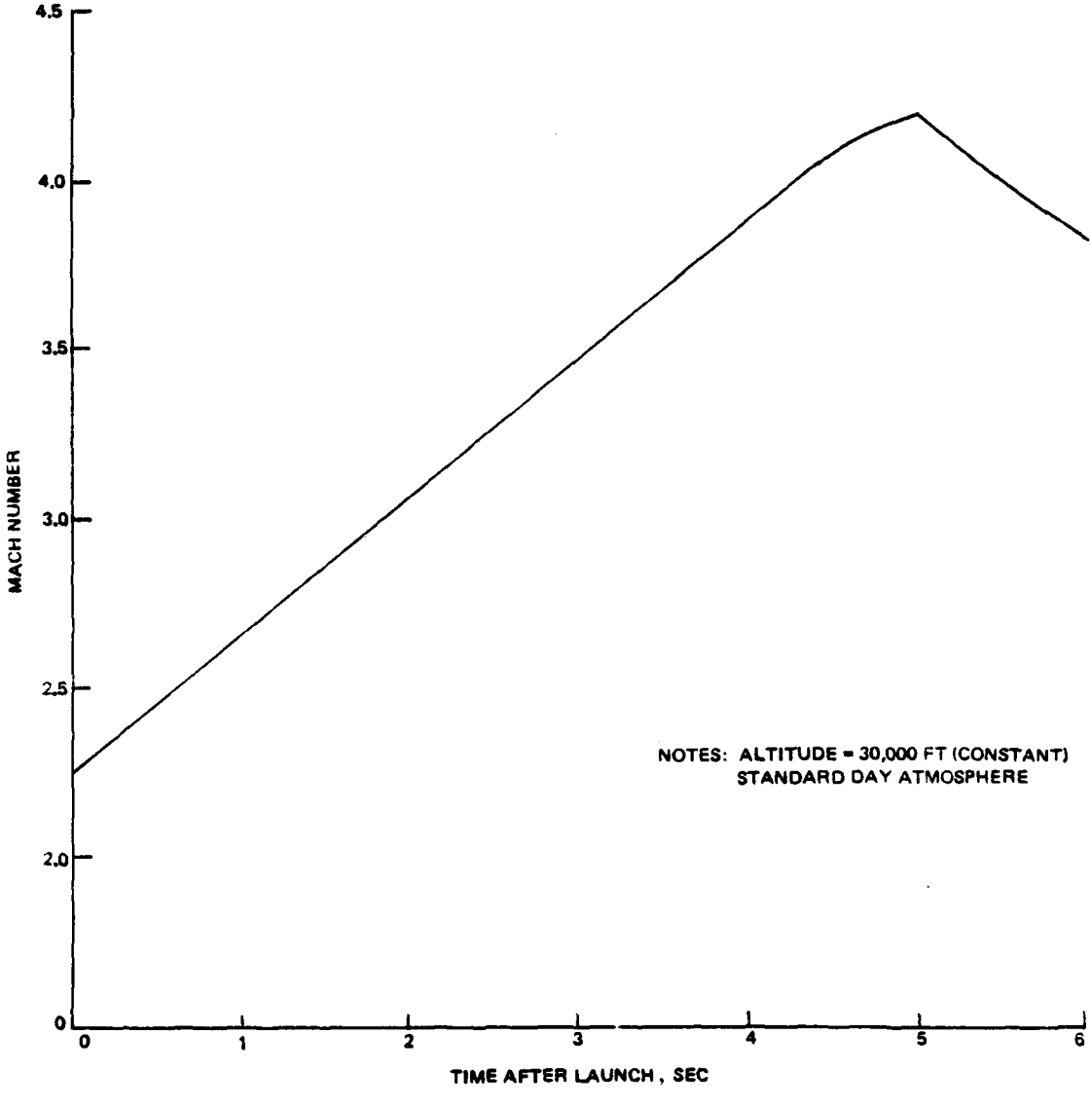

FIGURE 2. Free-Flight Profile.

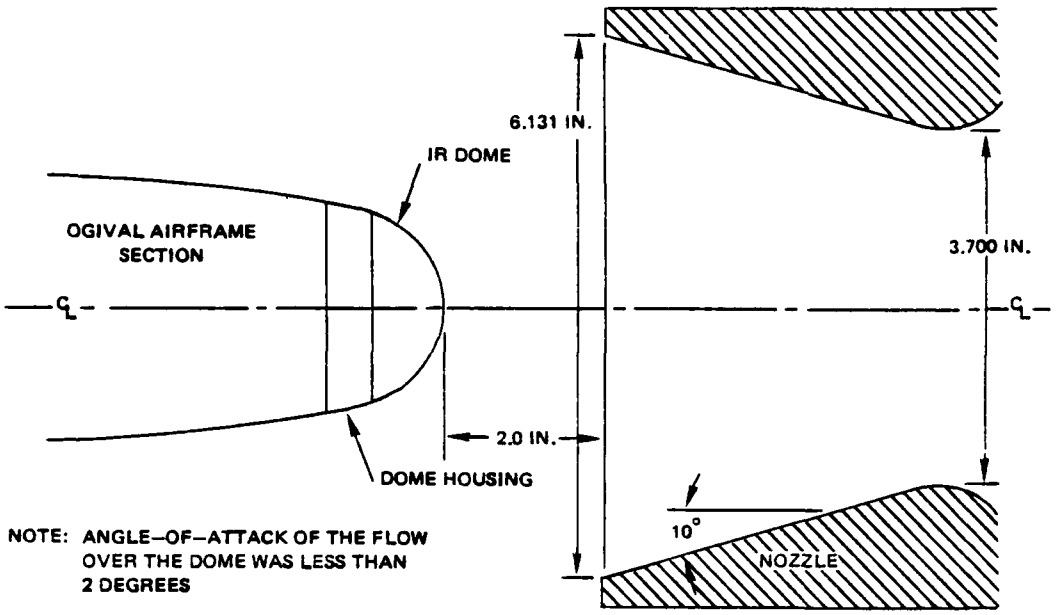

FIGURE 3. IR Dome Test Setup.

TABLE 1. Simulated Free-Flight Conditions.

Free-flight conditions					T-Range nozzle exit conditions			
t, sec	Mach no.	P_t, psia	T_t, °R	P_{t_2}, psia	Mach no.	P_t, psia	T_t, °R	P_{t_2}, psia
0	2.25	51	828	31	2.54	64	828	31
1	2.64	93	981	41	2.54	86	981	41
2	3.06	178	1170	55	2.53	114	1170	55
3	3.49	336	1386	71	2.52	147	1386	71
4	3.90	602	1613	88	2.51	182	1613	88
5	4.20	910	1791	102	2.50	210	1791	102
6	3.84	554	1579	85	2.51	176	1579	85

P_t = Total pressure upstream of normal shock

P_{t_2} = Total pressure downstream of normal shock

T_t = Total temperature

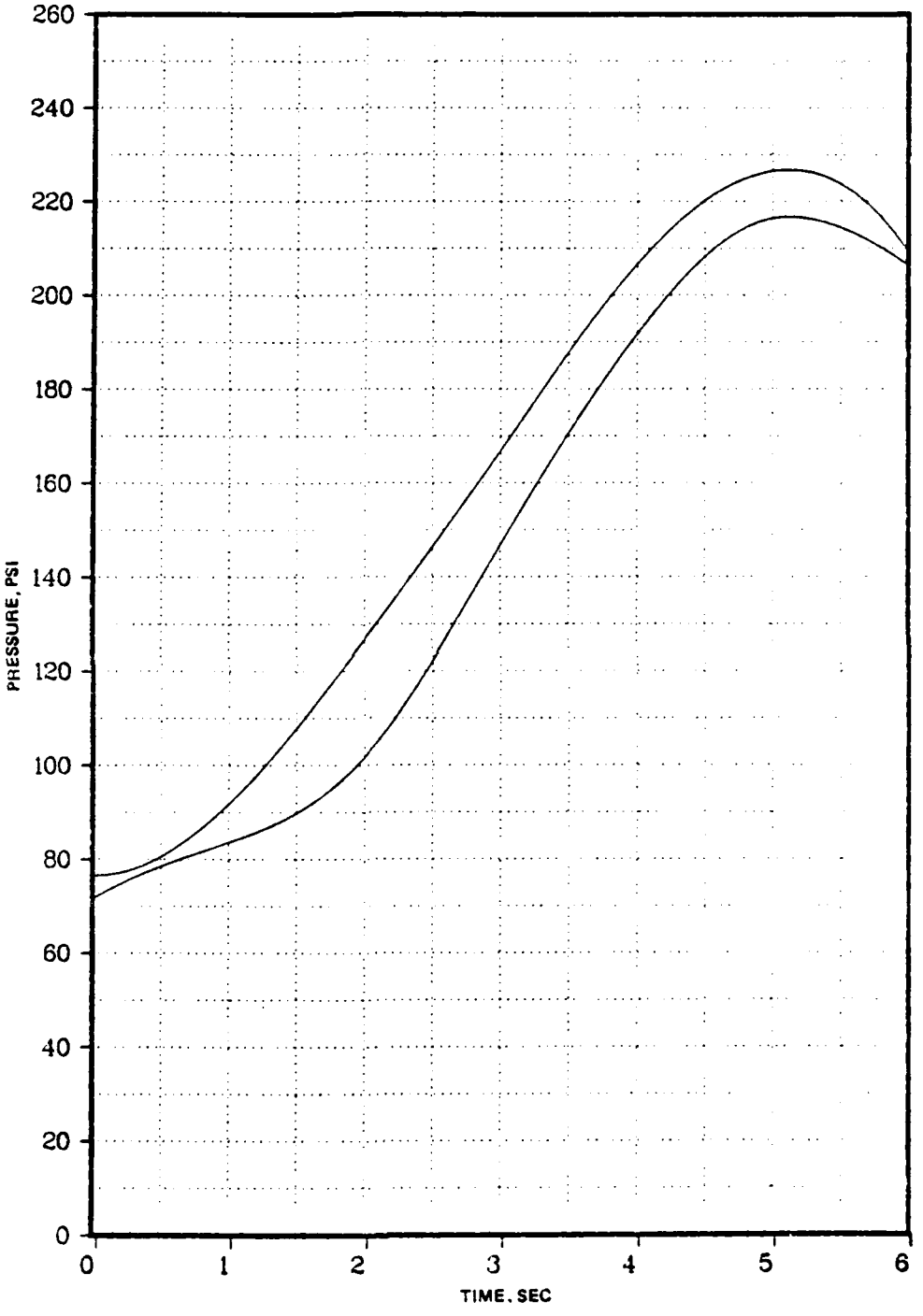

FIGURE 4. Free-Flight Simulation Total Pressure Profile Extremes.

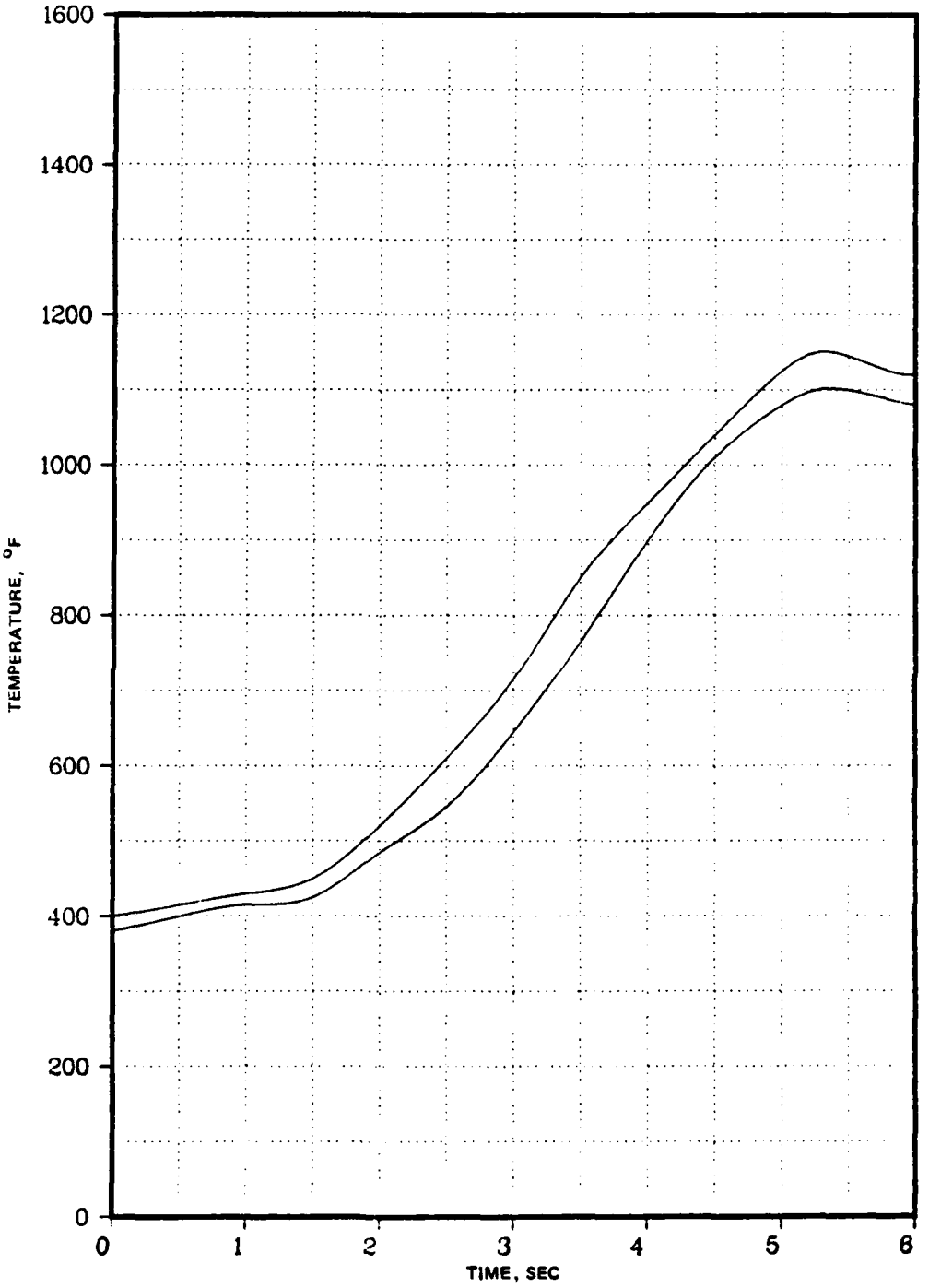

FIGURE 5. Free-Flight Simulation Total Temperature Profile Extremes.

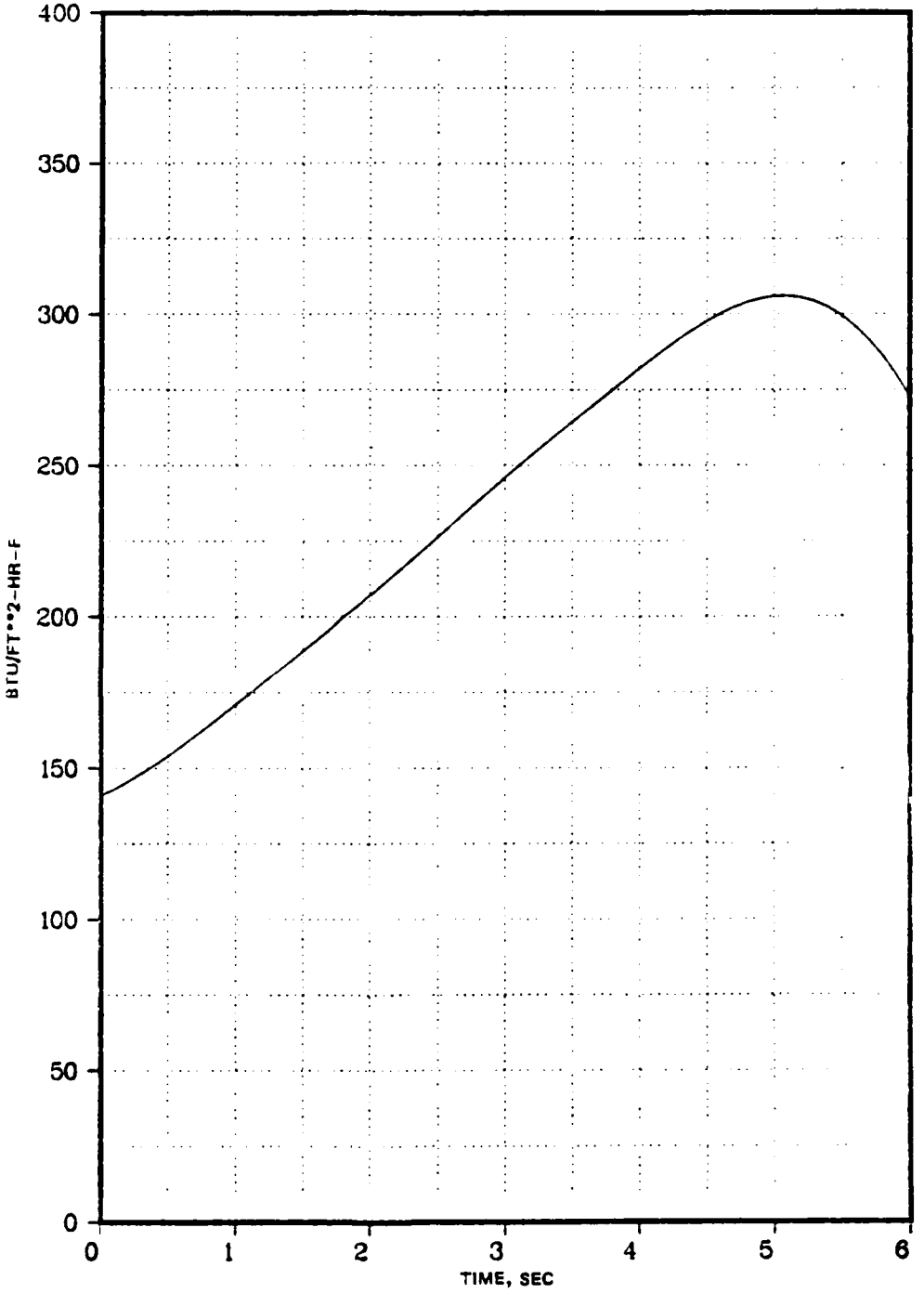

FIGURE 6. Stagnation Point Heat Transfer Coefficient Profile.

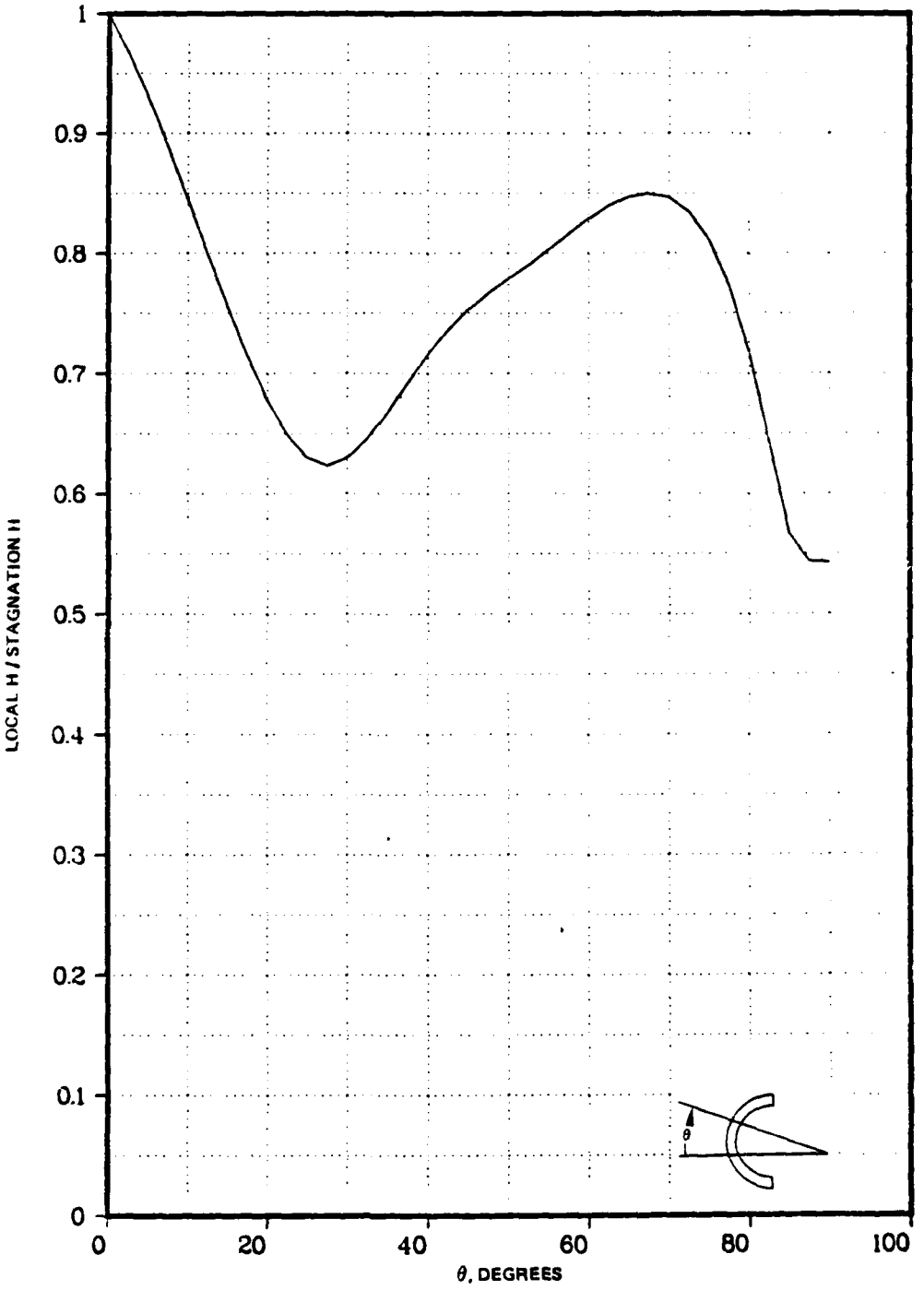

FIGURE 7. Streamwise Heat Transfer Coefficient Distribution.

Temperature and thermal stress levels within the MgF_2 domes during the simulated free flight were predicted from thermal and stress computer models[8,9] (see also footnote 1), and the observed total temperature and heat transfer coefficient profiles. The accuracy of the computer models have been verified experimentally in an earlier investigation (footnote 1). The predicted thermal stress profile corresponding to the time variation in facility total pressure and temperature is shown in Figure 8 for the dome stagnation point. The predicted streamwise variation of thermal stresses in the dome at the end of the free-flight boost phase is shown in Figure 9. It was found (see footnote 1) that the metal dome housing could be idealized by a simply supported dome rim with small loss of accuracy. The predominant effect of the housing on the dome stress distribution was to change the dome temperature distribution locally.

All of the MgF_2 domes fractured during the free-flight aerodynamic heating stimulation. Time to dome fracture after the simulated missile launch was obtained from 400 frame/second camera records of each dome test. The probability of MgF_2 dome fracture as a function of time after simulated missile launch is shown in Figure 10. All domes were subjected to a thermal environment corresponding to the Mach 2.25 launch condition for a minimum of 20 seconds prior to the start of the simulated free flight. Note that 50% of the domes failed within 4.5 seconds (Figure 10) at a corresponding stress of less than 10,000 psi (Figure 8). The published value of the mean fracture stress obtained from small material specimens is on the order of 20,000 psi.[10]

WEIBULL FRACTURE THEORY

The fracture theory developed by Weibull (see footnote 2) assumes that fracture occurs when the tensile stress exceeds the strength of the weakest flaw present in a material sample. It is further assumed that the flaws (type unspecified) occur in a manner such that the probability of fracture for the brittle material is described by the expression:

$$P_f = 1 - \exp\left[-\int_\eta \left(\frac{\sigma - \sigma_u}{\sigma_o}\right)^m d\eta\right]$$

[8] Naval Weapons Center. *Aerodynamic Heating of Spherically Tipped Cylinders, Cones and Ogives Using the General Thermal Analyzer SINDA*, by W. R. Compton. Cluna Lake, Calif., NWC, June 1974 (NWC TN 4061-172, publication UNCLASSIFIED.)

[9] The Aerospace Corporation. *SAAS-III Finite Element Stress Analysis of Axisymmetric and Plane Solids with Different Orthotropic, Temperature-Dependent Material Properties on Tension and Compression*, by R. M. Jones and J. G. Crose. Los Angeles, Calif., June 1971. (TR-0059 (56816-53)-1, publication UNCLASSIFIED.)

[10] The Eastman Kodak Company. *Kodak Irtran, Infrared Optical Materials*, 1971. (Kodak Publication U-72, UNCLASSIFIED.)

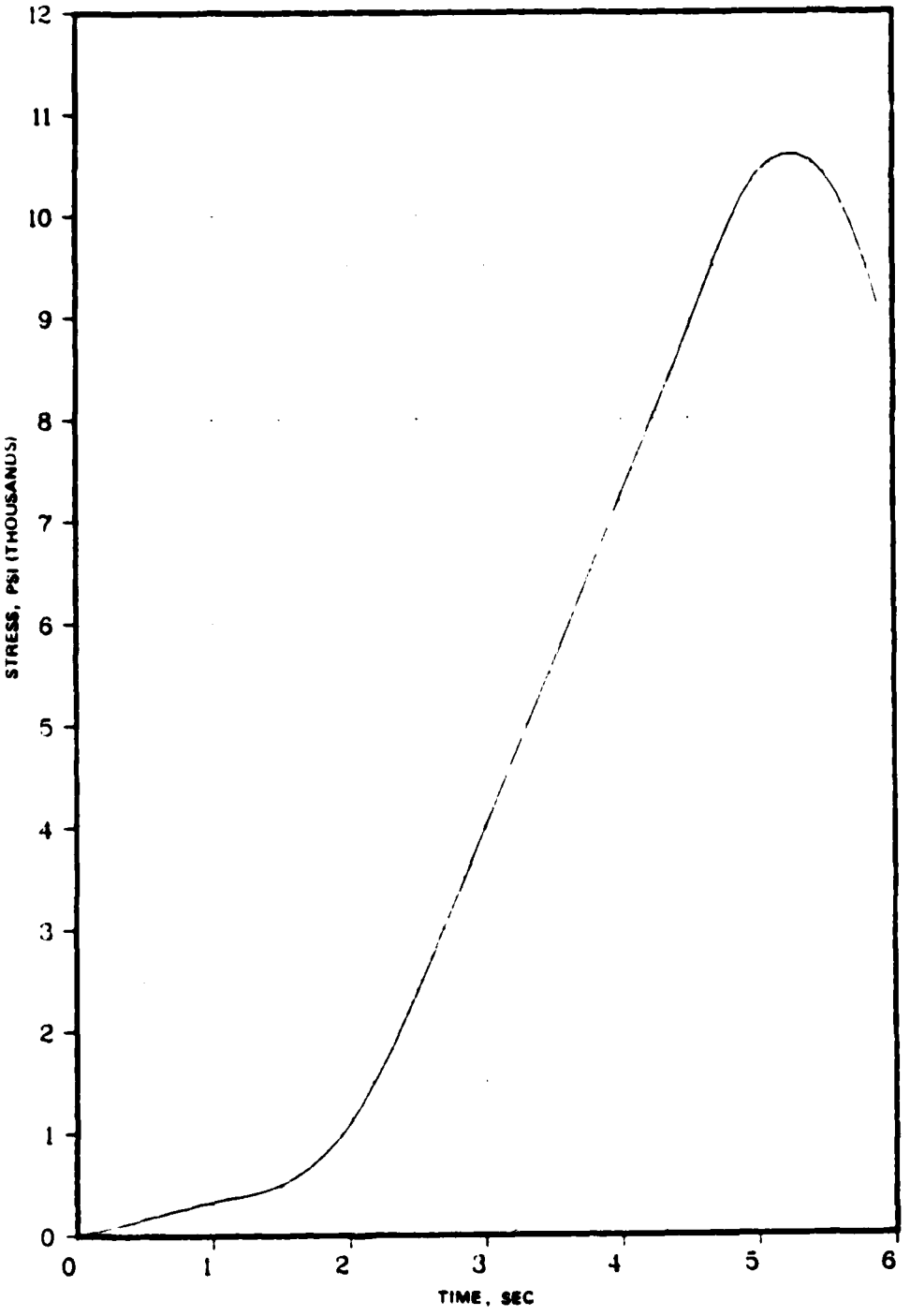

FIGURE 9. Stagnation Point Thermal Stress Profile.

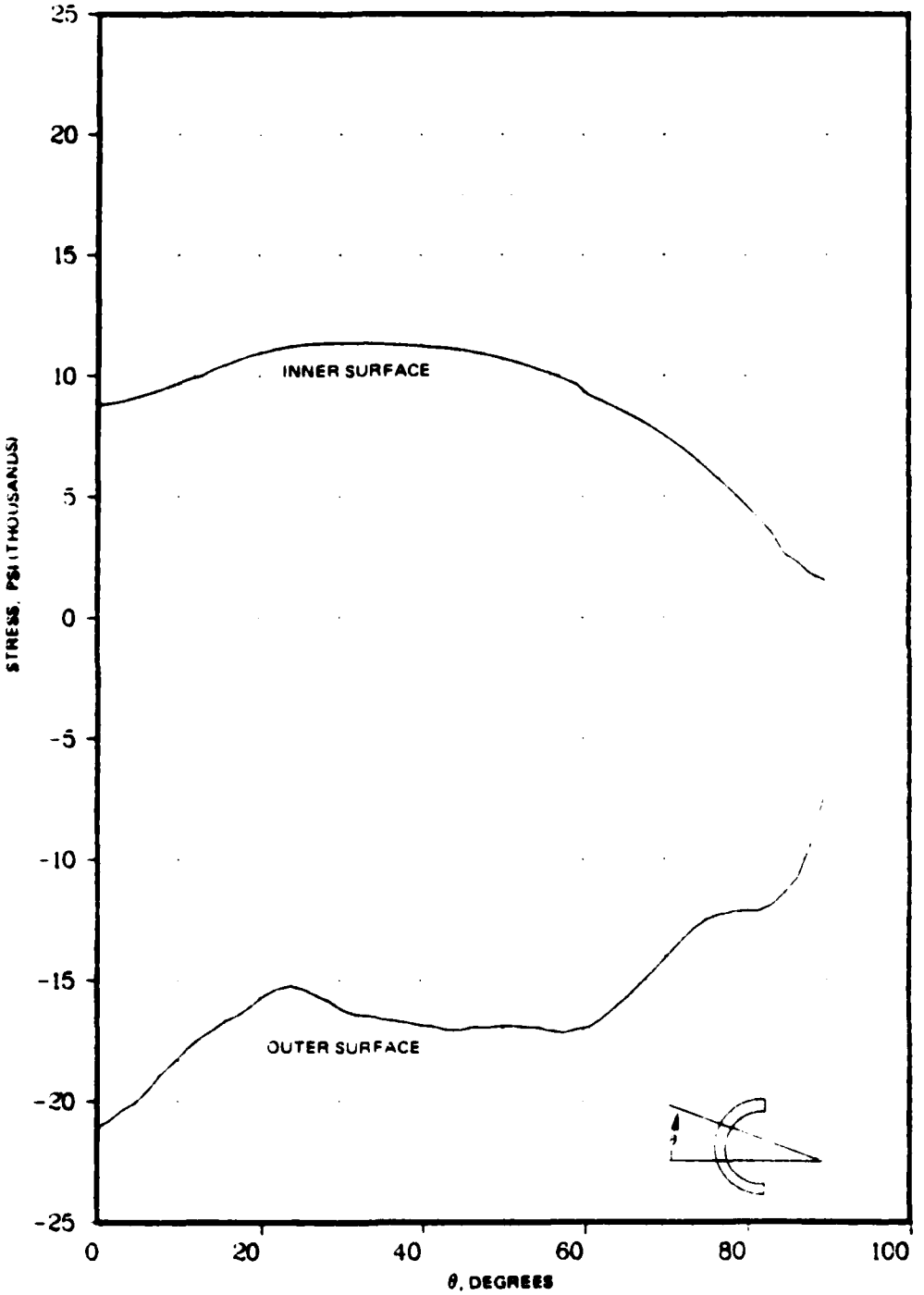

FIGURE 9. Streamwise Thermal Stress Distribution.

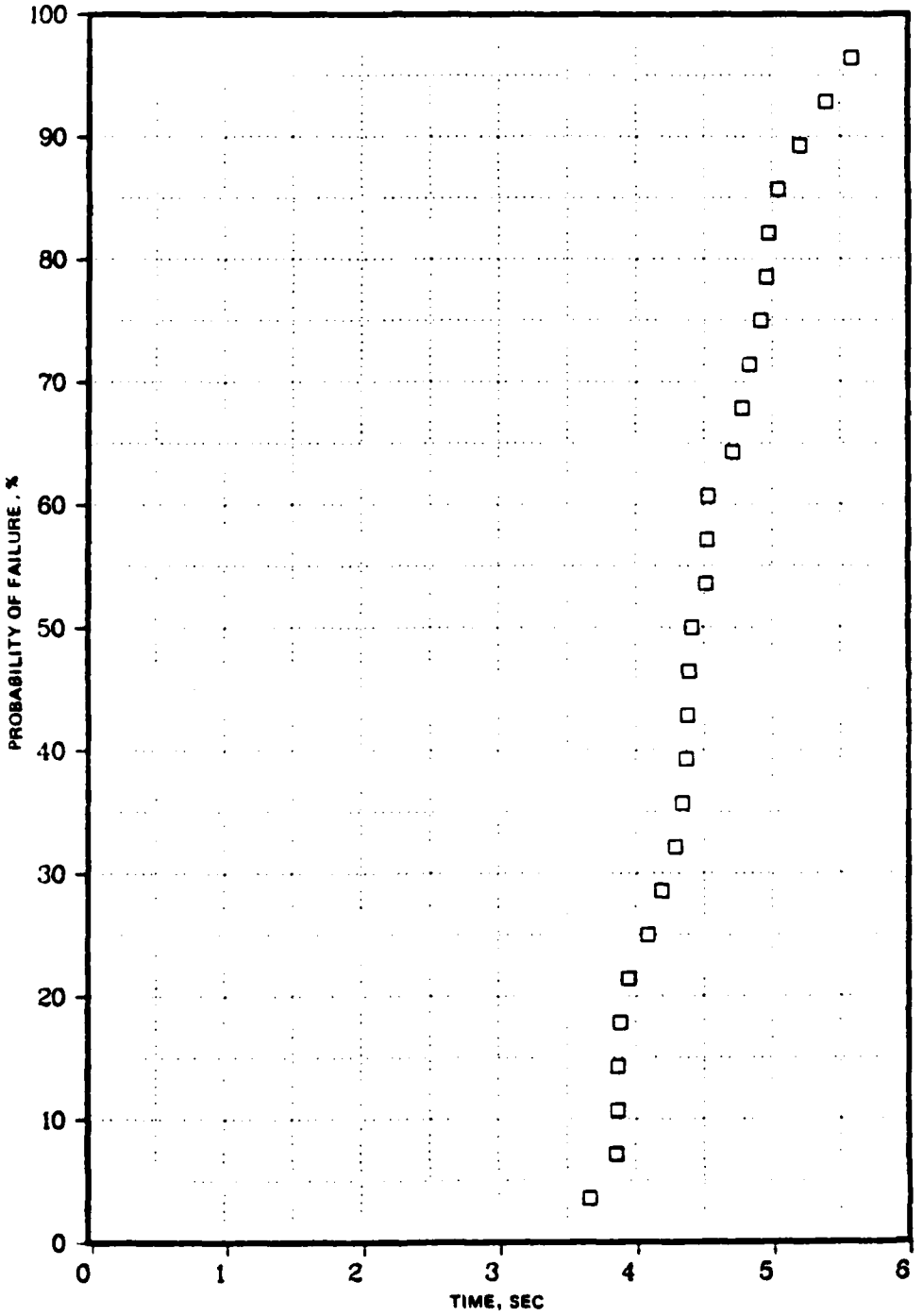

FIGURE 10. Experimental Probability of MgF_2 Dome Fracture.

where

P_f = probability of fracture

σ = applied tensile stress

σ_u = tensile stress at which $P_f = 0$

σ_o = a scaling parameter

m = a flaw density parameter

n = either the surface area or the volume of the material

The parameters σ_u, σ_o, and m are determined by a least-squares fit of the fracture strength data obtained from flexural strength tests (see footnote 3). The values of σ_o and m for MgF_2 have been determined using Weibull's two-parameter ($\sigma_u = 0$) method using the expressions below.

$$m = \frac{\sum_{n=1}^{N} X_n \sum_{n=1}^{N} Y_n - N \sum_{n=1}^{N} X_n Y_n}{\left[\sum_{n=1}^{N} X_n\right]^2 - N \sum_{n=1}^{N} X_n^2}$$

$$C = \frac{\sum_{n=1}^{N} X_n^2 \sum_{n=1}^{N} Y_n - \sum_{n=1}^{N} X_n Y_n}{N \sum_{n=1}^{N} X_n - \left[\sum_{n=1}^{N} X_n\right]^2}$$

$$\sigma_o = \exp\left\{\frac{1}{m}\left[\ln \frac{V}{2} - \ln (m + 1) - C\right]\right\} \qquad \text{Volume-distributed flaws}$$

$$\sigma_o = \exp\left\{\frac{1}{m}\left[\ln LW + \frac{LH}{m + 1} - C\right]\right\} \qquad \text{Surface-distributed flaws}$$

$$\ln P_s = \ln(1 - P_f) = - \frac{V}{2(m + 1)} \left(\frac{\sigma}{\sigma_o}\right)^m \qquad \text{Volume-distributed flaws}$$

$$\ln P_s = \ln(1 - P_f) = - \left[LW + \frac{LH}{m + 1}\right] \left(\frac{\sigma}{\sigma_o}\right)^m \qquad \text{Surface-distributed flaws}$$

where

H = material specimen thickness parallel to the applied load (Figure 11)

L = material specimen length between supports

V = material specimen volume between supports

W = material specimen width normal to the applied load

$X_n = \ell n \sigma_n$

$Y_n = \ell n \ell n \frac{n + 1}{n + 1 - n}$

n = number of material specimens that failed at a maximum tensile strength of σ_n or lower

N = total number of material specimens tested

σ_n = maximum tensile stress at fracture for the n^{th} material specimen

P_s = probability of survival

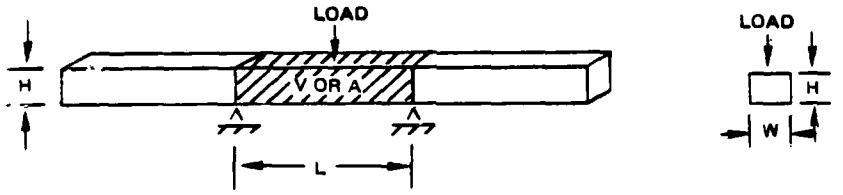

UNIAXIAL TEST SPECIMEN

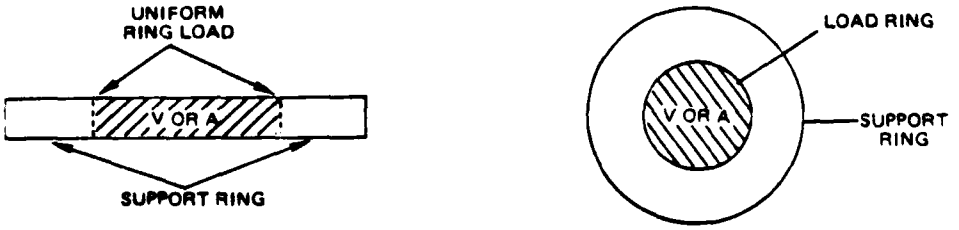

EQUIBIAXIAL TEST SPECIMEN

FIGURE 11. Material Specimen Geometry.

A summary of values for the Weibull parameters obtained for MgF_2 is given in Table 2. The fracture data[6] are the data obtained from flexural strength tests of material specimens with surface scratches less than $6(10)^{-4}$ inch (15 μm) deep. A comparison of the results of the least-squares approximation and the fracture strength data is shown in Figures 12 through 16.

The probability of fracture for a given dome geometry is determined as follows:

1. The temperature distribution within the dome is determined as a function of time.

2. The thermal stresses within the dome are determined at a particular time from the temperature distribution and a finite-element stress analysis.

3. The probability of survival, $P_s = 1 - P_f$, is determined for each volume (surface) element (Δn) in the stress model by using the maximum principal stress (tensile) in that element (σ), and the approximation,

$$P_s = \exp\left[- \Delta n \left(\frac{\sigma}{\sigma_o}\right)^m \right]$$

4. The probability of dome survival is then determined for that particular time by taking the product of the individual volume (surface) element probabilities of survival.

Weibull's method is widely used to predict brittle material fracture. There is, however, no theoretical way of demonstrating that the method is valid for materials that exhibit large fracture strength dispersions. Batdorf (see footnote 4) has demonstrated analytically that the physical model implied by Weibull's method is not satisfactory when the flaw density parameter, m, is greater than six.

TABLE 2. Uniaxial MgF_2 Fracture Data.

Temperature, °F	Volume theory, σ_o, psi	Surface theory, σ_o, psi	m
75	7,507	19,814	8.5
250	10,152	19,897	12.78
500	8,625	20,302	9.77
750	4,470	20,371	5.12
1000	2,279	17,269	3.75

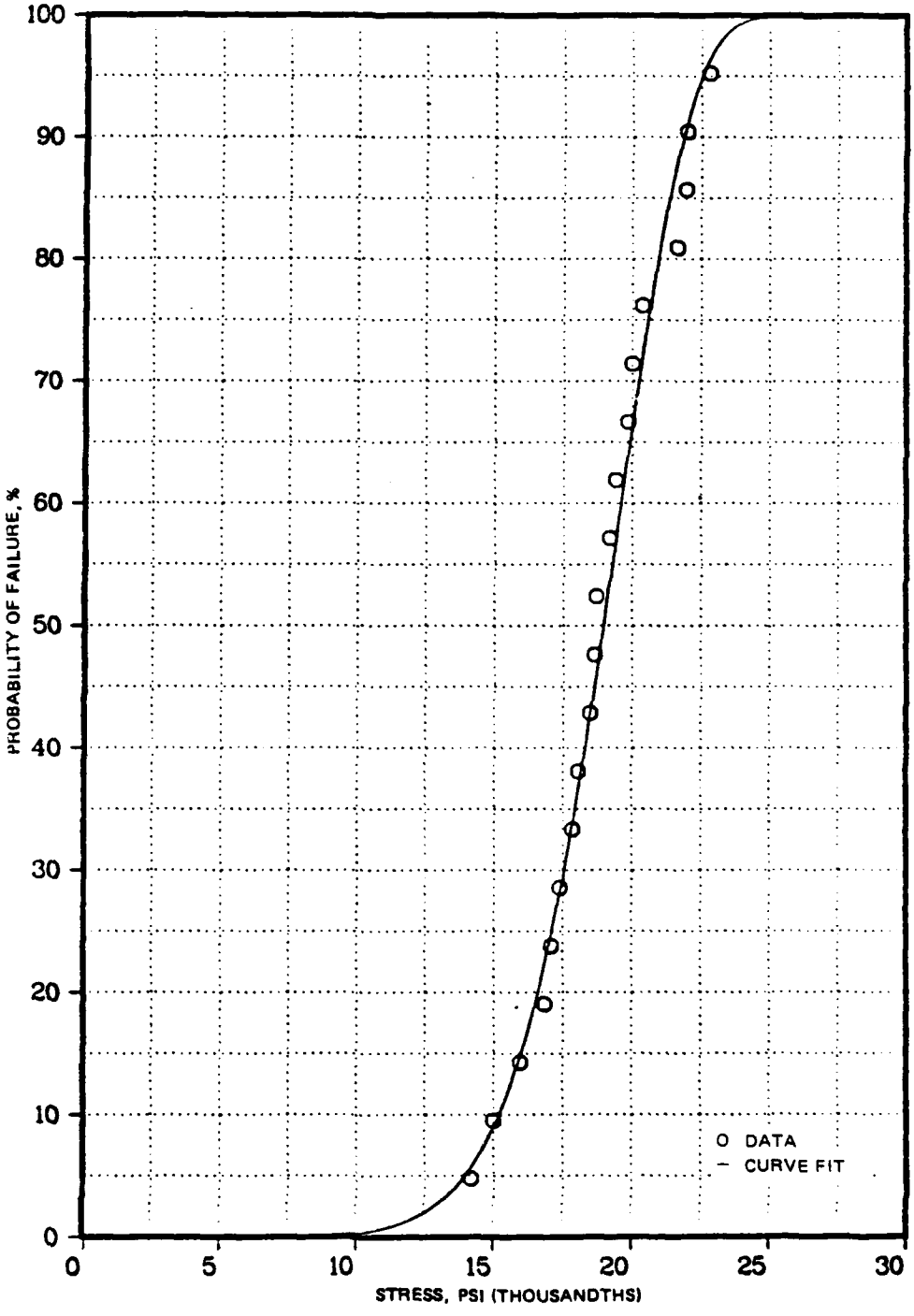

FIGURE 12. MgF_2 Uniaxial Fracture Statistics (T = 75°F).

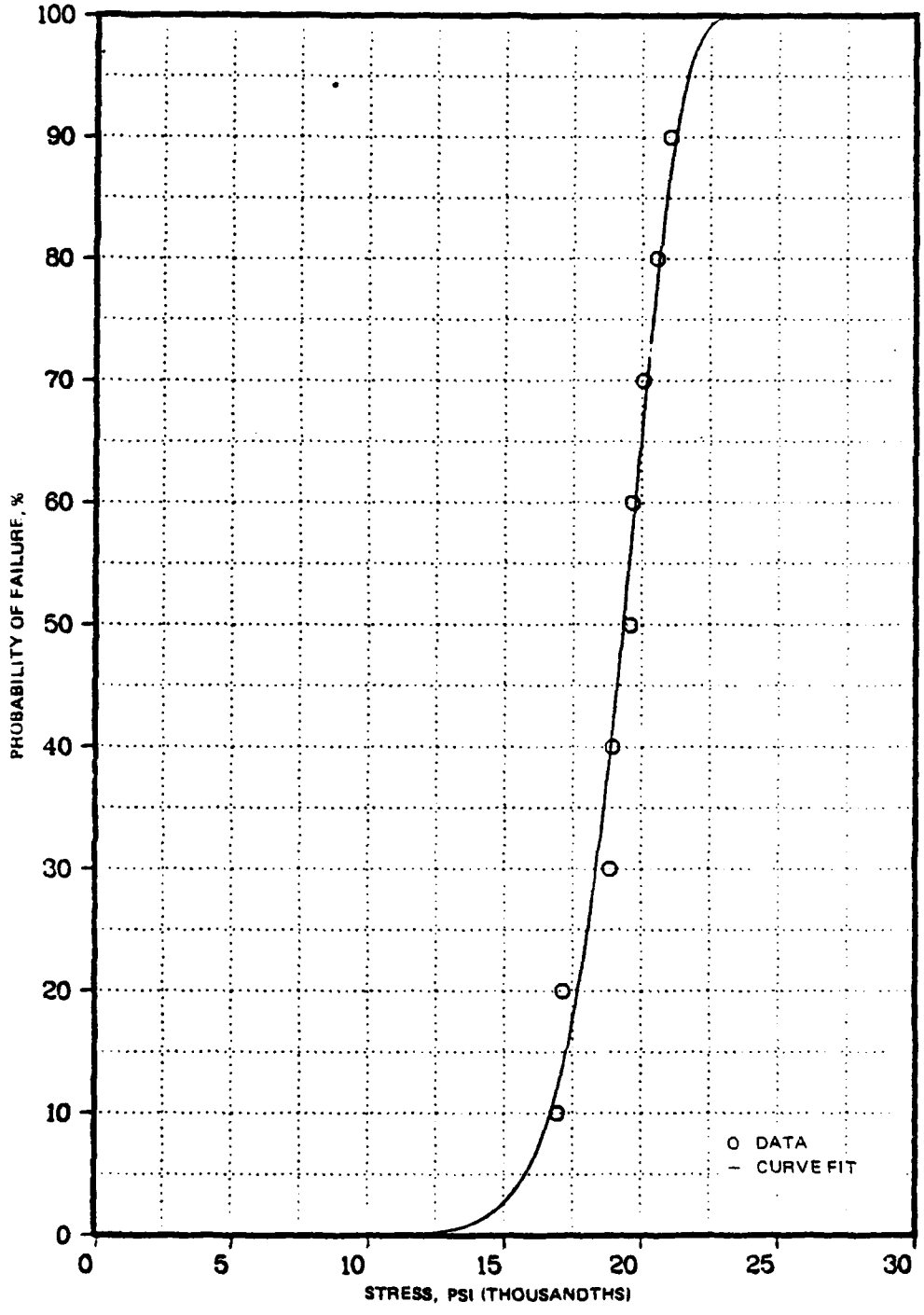

FIGURE 13. MgF_2 Uniaxial Fracture Statistics (T = 250°F).

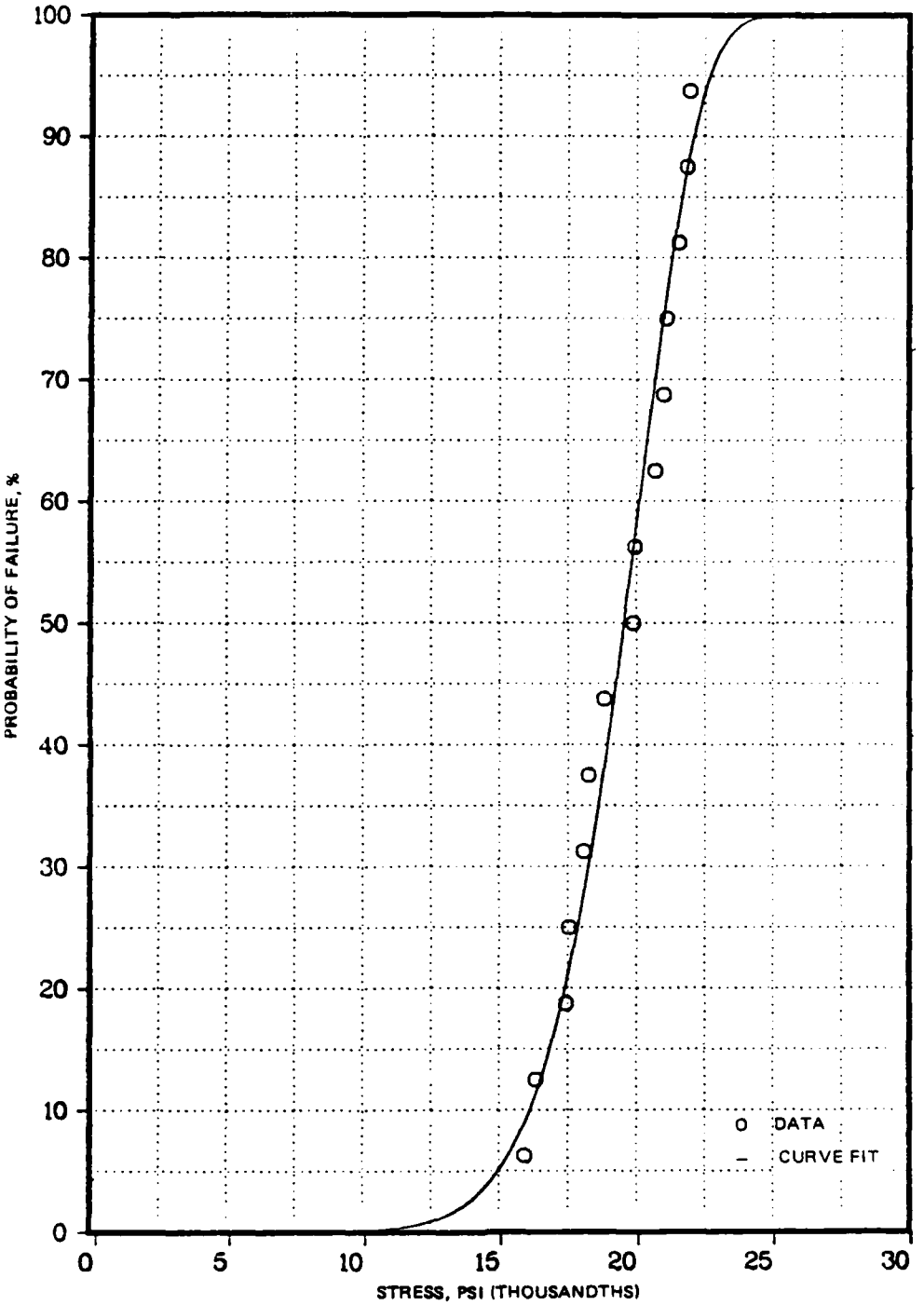

FIGURE 14. MgF_2 Uniaxial Fracture Statistics (T = 500°F).

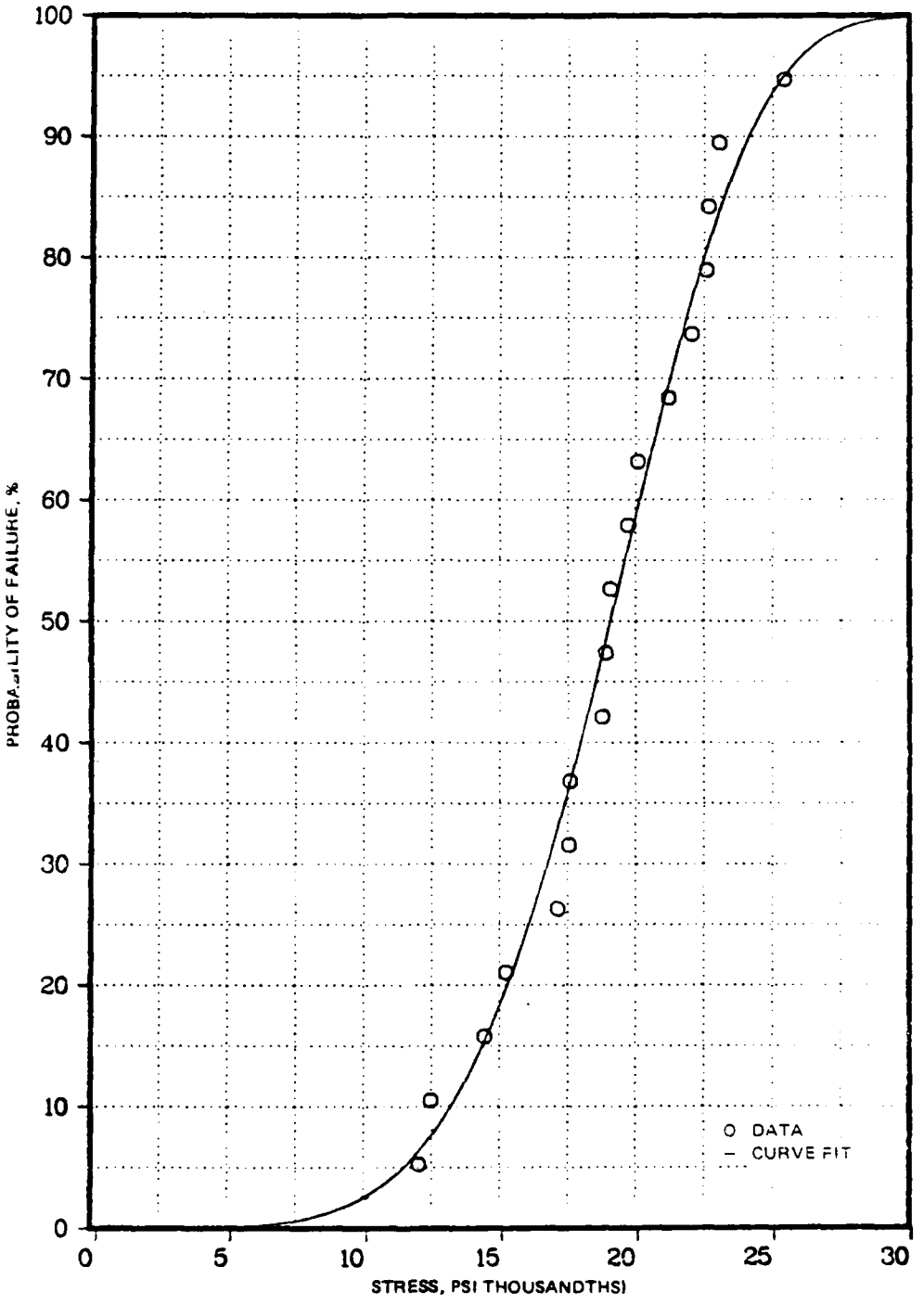

FIGURE 15. MgF_2 Uniaxial Fracture Statistics (T = 750°F).

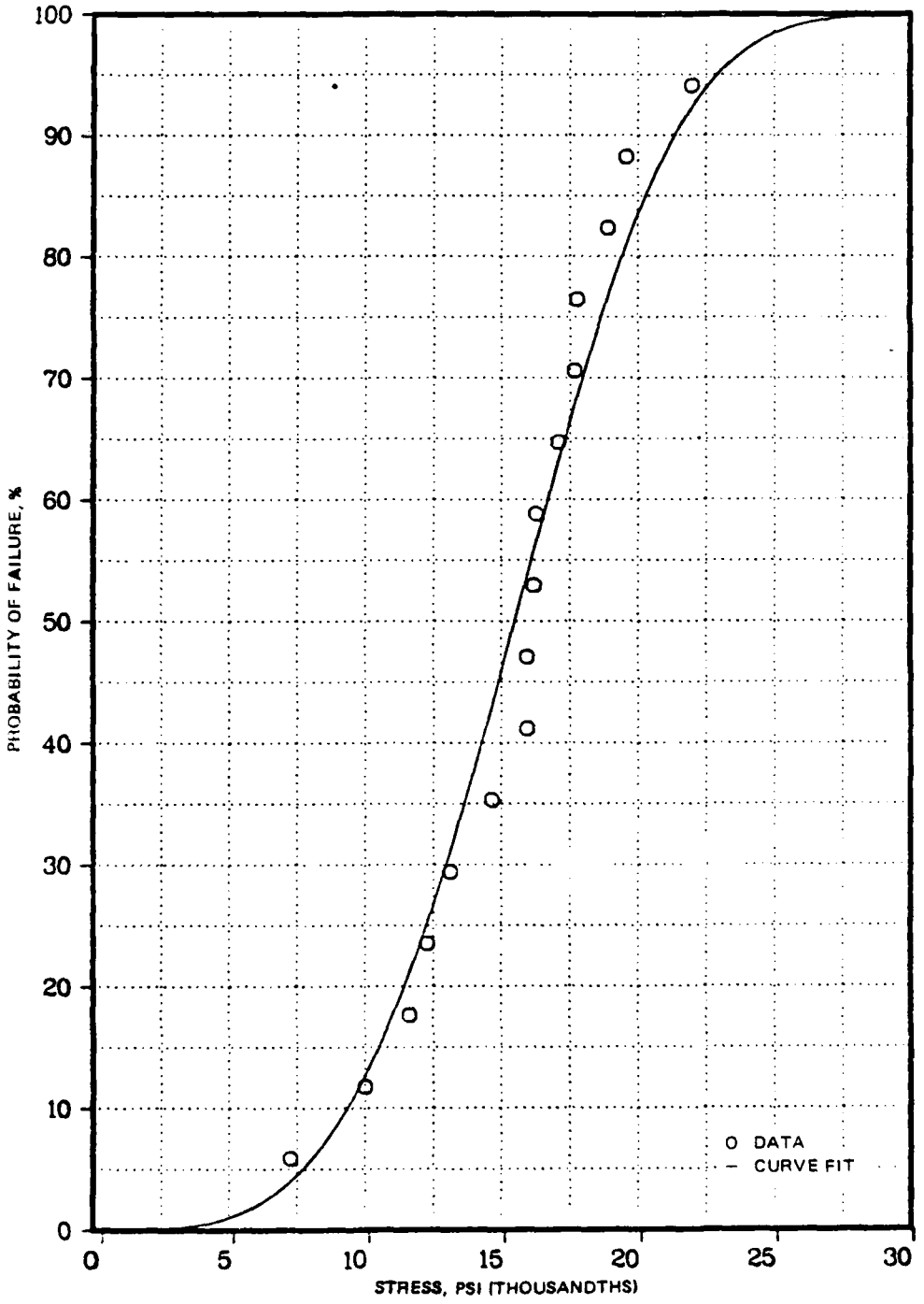

FIGURE 16. MgF_2 Uniaxial Fracture Statistics (T = 1000°F).

BATDORF FRACTURE THEORY

VOLUME-DISTRIBUTED CRACKS

The fracture theory developed by Batdorf (footnote 4) assumes that the flaws existing within a brittle material are penny-shaped intergranular cracks. In addition, Batdorf devised a means of accounting for the effects of crack orientation on the probability of fracture in triaxial stress states. Batdorf arrived at the following expression for the probability of survival for a small volume element at a uniform stress state:

$$\ln P_s = -\int dV \int \frac{\Omega}{4\pi} \frac{dM}{d\sigma_c} d\sigma_c$$

$$= -\int dV \int \frac{\Omega}{4\pi} dM$$

$$\cong -\Delta V \int \frac{\Omega}{4\pi} dM$$

where

M = probability that a crack of critical strength σ_c (or less) is present in the volume element (ΔV)

$\frac{\Omega}{4\pi}$ = probability that the crack is oriented in a direction such that the stress normal to the crack plane exceeds the critical crack strength

σ_c = crack critical strength

The probability that the crack is oriented in a direction that will result in fracture is determined from the expression,

$$\frac{\Omega}{4\pi} = 1 - \frac{2}{\pi} \int_0^{\frac{\pi}{2}} \cos\theta_c \, d\phi$$

where

$$\cos^2 \theta_c = \frac{K_c - \left[K_y - (K_y - K_z)\sin^2 \phi\right]}{1 - \left[K_y - (K_y - K_z)\sin^2 \phi\right]} \quad \text{(shear insensitive cracks)}$$

$$\cos^2 \theta_c = \frac{K_c^2 - \left[K_y - (K_y - K_z)\sin^2 \phi\right]^2}{1 - \left[K_y - (K_y - K_z)\sin^2 \phi\right]^2} \quad \text{(shear sensitive cracks)}$$

$K_c = \sigma_c/\sigma_x$

$K_y = \sigma_y/\sigma_x$

$K_z = \sigma_z/\sigma_x$

ϕ = angle between the component of σ_N in the $\sigma_y - \sigma_z$ plane and the σ_y axis (Figure 17)

θ = angle between σ_N and the σ_x axis

σ_N = stress resulting from the principal stresses in a direction normal to the plane of the crack

σ_x = principal stress in the x direction

σ_y = principal stress in the y direction

σ_z = principal stress in the z direction

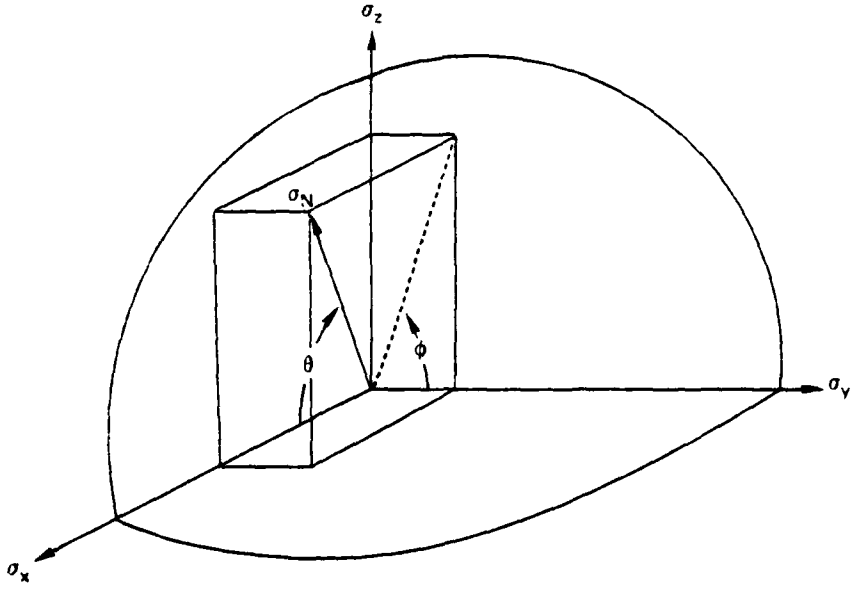

FIGURE 17. Volume-Distributed Crack Coordinate System.

The preceding integral has been evaluated for the following stress states:

Shear Insensitive Cracks

$(K_y = 0, K_z = 0)$

$$\frac{\Omega}{4\pi} = 1 - \sqrt{K_c} \qquad \text{(uniaxial)}$$

$(K_y = 1, K_z = 0)$

$$\frac{\Omega}{4\pi} = \sqrt{1 - K_c} \qquad \text{(equibiaxial)}$$

$(K_y = 1, K_z = 1)$

$$\frac{\Omega}{4\pi} = 1 \qquad \text{(equitriaxial)}$$

$(K_z \leq K_c \leq K_y)$

$$\frac{\Omega}{4\pi} = \left[1 - \frac{(1 - K_y)(K_c - K_z)}{(1 - K_c)(K_y - K_z)}\right]\sqrt{\frac{1 - K_c}{1 - K_z}} + \frac{2}{\pi}\frac{(1 - K_y)(K_c - K_z)}{(1 - K_c)(K_y - K_z)}\sin^{-1}\sqrt{\frac{1 - K_c}{1 - K_z}} \qquad \text{(triaxial)*}$$

$(K_y \geq K_c \leq 1)$

$$\frac{\Omega}{4\pi} = 1 - \left[1 - \frac{(1 - K_c)(K_y - K_z)}{(1 - K_y)(K_c - K_z)}\right]\sqrt{\frac{K_c - K_z}{1 - K_z}} - \frac{2}{\pi}\frac{(1 - K_c)(K_y - K_z)}{(1 - K_y)(K_c - K_z)}\sin^{-1}\sqrt{\frac{K_c - K_z}{1 - K_z}} \qquad \text{(triaxial)*}$$

*See Appendix A.

Shear Sensitive Cracks

$(K_y = 0, K_z = 0)$

$$\frac{\Omega}{4\pi} = 1 - K_c \qquad \text{(uniaxial)}$$

$(K_y = 1, K_z = 0)$

$$\frac{\Omega}{4\pi} = \sqrt{1 - K_c^2} \qquad \text{(equibiaxial)}$$

$(K_y = 1, K_z = 1)$

$$\frac{\Omega}{4\pi} = 1 \qquad \text{(equitriaxial)}$$

Evaluation of the integral for $\Omega/4\pi$ for shear sensitive cracks in a triaxial stress state involves rather messy hyperelliptic integrals and is best treated via numerical integration techniques.

If the critical crack strength parameter, M, is expressed as a series,

$$M = \sum_{n=1} a_n \sigma_c^n = \sum_{n=1} a_n \sigma_x^n K_c^n$$

then the probability of survival can be determined analytically for the following special cases:

Shear Insensitive Cracks

$$\ln P_s = -V \sum_{n=1} \frac{a_n \sigma_m^n}{(2n + 1)} \qquad \text{(uniaxial, pure tension)}$$

$$\ln P_s = -\frac{V}{2} \sum_{n=1} \frac{a_n \sigma_m^n}{(n + 1)(2n + 1)} \qquad \text{(uniaxial, pure bending)}$$

$$\ln P_s = -\frac{V}{2} \sum_{n=1} \frac{n a_n \sigma_m^n}{(n + 1)} B\left(n, \frac{3}{2}\right) \qquad \text{(equibiaxial, pure bending)}$$

Shear Sensitive Cracks

$$\ell nP_s = -V \sum_{n=1} \frac{a_n \sigma_m^n}{(n+1)} \qquad \text{(uniaxial, pure tension)}$$

$$\ell nP_s = -\frac{V}{2} \sum_{n=1} \frac{a_n \sigma_m^n}{(n+1)^2} \qquad \text{(uniaxial, pure bending)}$$

$$\ell nP_s = -\frac{V}{4} \sum_{n=1} \frac{n a_n \sigma_m^n}{(n+1)} B\left(\frac{n}{2}, \frac{3}{2}\right) \qquad \text{(equibiaxial, pure bending)}$$

where

σ_m = maximum tensile stress

B = Beta function

The coefficients, a_n, in the preceding series are determined from material specimens by fitting a least-squares polynomial to the fracture data:

$$\ell nP_s = \ell n \left[\frac{N+1-n}{N+1}\right] = -\sum_{i=1} b_i \sigma_m^i$$

If four-point bending tests have been used, for example, then the a_n coefficients can be expressed in terms of the b_n coefficients of the least-squares fit to the fracture data.

$$a_n = 2(n+1)(2n+1)\frac{b_n}{V} \qquad \text{(uniaxial, shear insensitive)}$$

$$a_n = 2(n+1)^2 \frac{b_n}{V} \qquad \text{(uniaxial, shear sensitive)}$$

The probability of survival of a material volume element in a triaxial stress state can then be expressed,

$$\ell nP_s = -\Delta V \int_o^1 \frac{\Omega}{4\pi} \sum_{n=1} n a_n \sigma_x^n K_c^{n-1} dK_c$$

where σ_x is the maximum principal stress (tension) in the volume element and $\Omega/4\pi$ is determined from the stress state that exists within the element. The probability of dome survival is then determined in the same way as described for Weibull's fracture theory.

The current investigation employed a simplified version of the above equations. The analysis was constrained to using shear sensitive cracks and the critical crack strength parameter, M, was simplified to

$$M = (m + 1)\left(\frac{\sigma_x}{\sigma_o}\right)^m K_c^m$$

where m and σ_o are the Weibull parameters. The parameters, m and c, are determined from the equations given in the section describing the Weibull fracture theory. The parameter, σ_o, is determined from the following relations:

$$\sigma_o = \exp\left\{\frac{1}{m}\left[\ell nV - C\right]\right\} \qquad \text{(uniaxial, pure tension)}$$

$$\sigma_o = \exp\left\{\frac{1}{m}\left[\ell n\,\frac{V}{2} - \ell n(m + 1) - C\right]\right\} \qquad \text{(uniaxial, pure bending)}$$

$$\sigma_o = \exp\left\{\frac{1}{m}\left[\ell n\,\frac{V}{4} + \ell nm + \ell nB\left(\frac{m}{2},\frac{3}{2}\right) - C\right]\right\} \qquad \text{(equibiaxial, pure bending)}$$

The probability of survival for these special cases then becomes,

$$\ell nP_s = -V\left(\frac{\sigma}{\sigma_o}\right)^m \qquad \text{(uniaxial, pure tension)}$$

$$\ell nP_s = -\frac{V}{2(m + 1)}\left(\frac{\sigma}{\sigma_o}\right)^m \qquad \text{(uniaxial, pure bending)}$$

$$\ell nP_s = -\frac{mV}{4} B\left(\frac{m}{2},\frac{3}{2}\right)\left(\frac{\sigma}{\sigma_o}\right)^m \qquad \text{(equibiaxial, pure bending)}$$

and the probability of survival for a volume element in a triaxial stress state is found by numerical integration of the expression,

$$\ell nP_s = -\Delta V(m + 1)\left(\frac{\sigma_x}{\sigma_o}\right)^m K_z^m - \Delta V\int_{K_z}^{1} m(m + 1)\left(\frac{\sigma_x}{\sigma_o}\right)^m \frac{\Omega}{4\pi} K_c^{m-1} dK_c$$

where $\Omega/4\pi$ is evaluated for the stress state existing within the volume element. The probability of dome survival is found by the method previously described in the section on the Weibull fracture theory.

The simplified method described above reduces to Weibull's method for uniaxial stress states, yet retains crack orientation effects on the probability of fracture in biaxial and triaxial stress states. In addition, the least-squares curve fit of the material specimen fracture data is identical to that used in the Weibull theory for uniaxial fracture tests. Consequently, the values for the parameters, m and σ_o, shown in Table 2 for uniaxial fracture data for MgF_2 can be used directly in the Batdorf fracture theory. Application of the simplified method to equibiaxial fracture data (see footnote 7) for MgF_2 leads to the values for m and σ_o shown in Table 3. A comparison between the least-squares fit approximation and the equibiaxial fracture data for MgF_2 is shown in Figure 18.

TABLE 3. Equibiaxial MgF_2 Fracture Data.

Temperature	75°F
Volume, σ_o	6,524 psi
Surface, σ_o	19,379 psi
m	4.318

SURFACE DISTRIBUTED CRACKS

The fracture theory developed by Batdorf (footnote 5) for surface flaws assumes that such flaws are cracks oriented normal to the surface. The effects of crack orientation on probability of fracture in a biaxial stress state are also included in the theory. The following expression is used to determine the probability of survival for a small surface area element in a uniform biaxial stress state:

$$\ell n P_s = -\int dA \int \frac{\omega}{\pi} \frac{dM}{d\sigma_c} d\sigma_c$$

$$= -\int dA \int \frac{\omega}{\pi} dM$$

$$= -\Delta A \int M d\left(\frac{\omega}{\pi}\right)$$

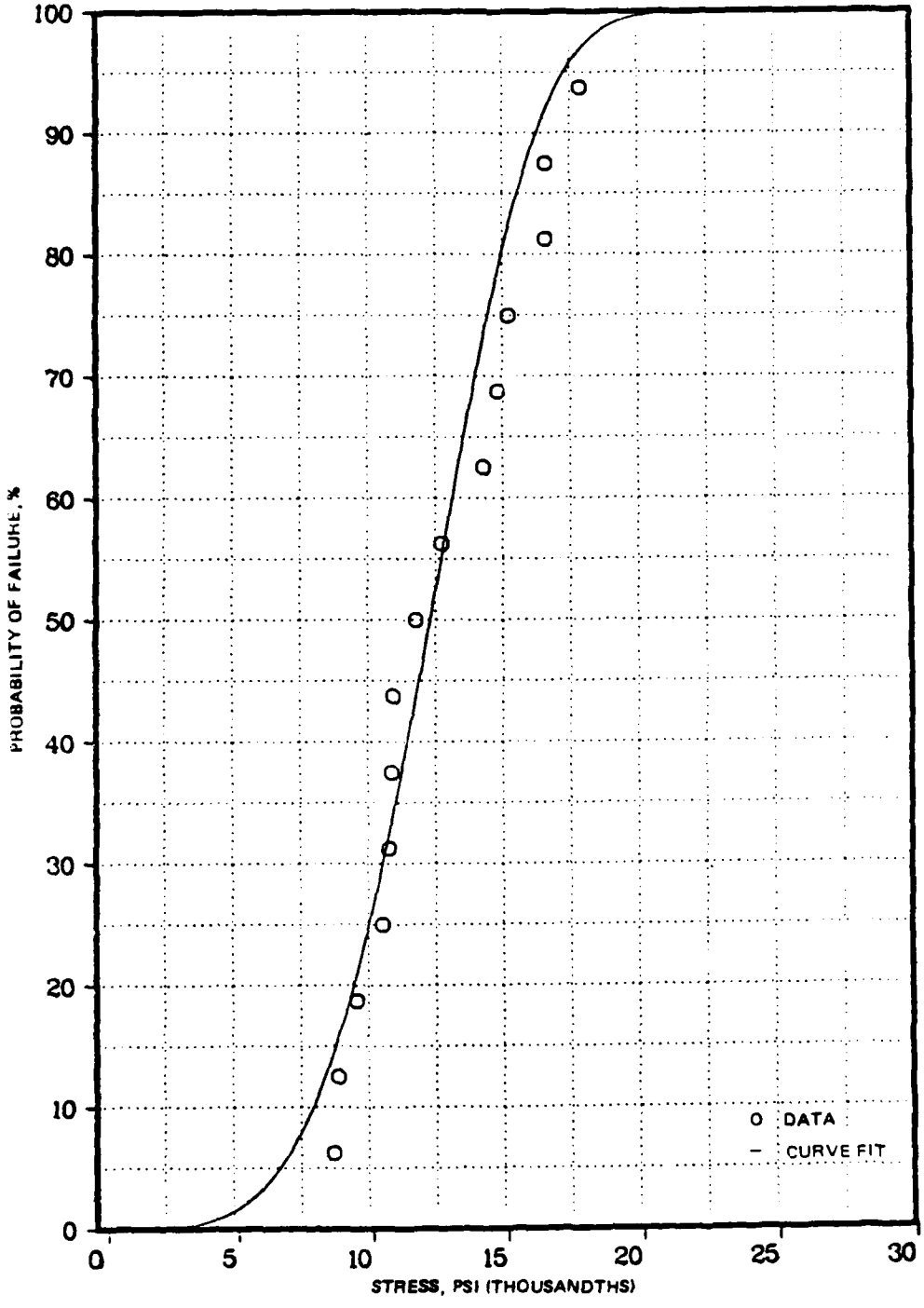

FIGURE 18. MgF_2 Equibiaxial Fracture Statistics (T = 75°F)

where

M = probability that a crack of critical strength σ_c (or less) is present in the surface area element (ΔA)

$\frac{\omega}{\pi}$ = probability that the crack is oriented in a direction such that the stress normal to the crack plane exceeds the critical crack strength

σ_c = critical crack strength

The probability that the crack is oriented in a direction that will result in fracture is determined by setting $\phi = 0$ in the expression for $\cos^2 \theta_c$ in the section on the volume-distributed crack theory.

$$\sin \theta_c = \sqrt{\frac{1 - K_c}{1 - K_y}} \qquad \text{(shear insensitive cracks)}$$

$$\sin \theta_c = \sqrt{\frac{1 - K_c^2}{1 - K_y^2}} \qquad \text{(shear sensitive cracks)}$$

Since ω must be equal to twice θ_c (Figure 19),

$$\frac{\omega}{\pi} = \frac{2}{\pi} \sin^{-1} \sqrt{\frac{1 - K_c}{1 - K_y}} \qquad \text{(shear insensitive cracks)}$$

$$\frac{\omega}{\pi} = \frac{2}{\pi} \sin^{-1} \sqrt{\frac{1 - K_c^2}{1 - K_y^2}} \qquad \text{(shear sensitive cracks)}$$

$$\frac{\omega}{\pi} = 1 \qquad \text{(equibiaxial limiting value)}$$

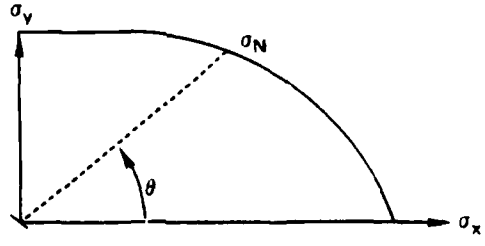

FIGURE 19. Surface-Distributed Crack Coordinate System.

If the critical crack strength parameter, M, is again expressed in series form,

$$M = \sum_{n=1} a_n \sigma_c^n = \sum_{n=1} a_n \sigma_x^n K_c^n$$

then the probability of survival can be determined analytically for the following cases:

Shear Insensitive Cracks

$$\ell n P_s = - \frac{2L}{\pi} [W + H] \sum_{n=1} a_n \sigma_m^n B \left(\frac{(2n + 1)}{2}, \frac{1}{2} \right)$$

(uniaxial, pure tension)

$$\ell n P_s = - \frac{1}{\pi} \sum_{n=1} \left[LW + \frac{LH}{n + 1} \right] a_n \sigma_m^n B \left(\frac{2n + 1}{2}, \frac{1}{2} \right)$$

(uniaxial, pure bending)

$$\ell n P_s = - A \sum_{n=1} a_n \sigma_m^n$$

(equibiaxial, pure bending)

Shear Sensitive Cracks

$$\ell n P_s = - \frac{2L}{\pi} [W + H] \sum_{n=1} a_n \sigma_m^n B \left(\frac{n + 1}{2}, \frac{1}{2} \right)$$

(uniaxial, pure tension)

$$\ell n P_s = - \frac{1}{\pi} \sum_{n=1} \left[LW + \frac{LH}{n + 1} \right] a_n \sigma_m^n B \left(\frac{n + 1}{2}, \frac{1}{2} \right)$$

(uniaxial, pure bending)

$$\ell n P_s = - A \sum_{n=1} a_n \sigma_m^n$$

(equibiaxial, pure bending)

The a_n coefficients are again determined from a least-squares fit to the fracture data. However, for the surface distributed crack theory, a solution can be obtained for any biaxial stress state* from the following:

Shear Insensitive Cracks

$$\ell n P_s = - \frac{\Delta A}{\pi} \sum_{n=1} a_n \sigma_x^n I_n$$

*See Appendix B

where

$$I_o = \frac{1}{\sqrt{-c}} \left[\sin^{-1} \left(\frac{-2cx - b}{\sqrt{b^2 - 4ac}} \right) \right]_{K_y}^{1} \qquad (K_y \leq x \leq 1)$$

$$I_1 = - \frac{b}{2c} I_o$$

$$I_2 = - \frac{\left(3b^2 - 4ac\right)}{8c^2} I_o$$

$$I_3 = \left(\frac{3ab}{4c^2} - \frac{5b^3}{16c^3} \right) I_o$$

$$\vdots$$

$$I_n = - \frac{(2n - 1)}{n} \frac{b}{2c} I_{n-1} - \frac{(n - 1)}{n} \frac{a}{c} I_{n-2}$$

$$a = -K_y$$

$$b = 1 + K_y$$

$$c = -1$$

Shear Sensitive Cracks

$$\ln P_s = - \frac{2\pi A}{\pi} \sum_{n=1} a_n x^n G_{n+1}$$

where

$$G_0 = \kappa(k)$$

$$G_1 = \frac{\pi}{2}$$

$$G_2 = \varepsilon(k)$$

$$G_3 = \frac{\pi}{4} \left[1 + K_y^2\right]$$

$$G_4 = - \frac{1}{3} K_y^2 \kappa(k) + \frac{2}{3} \left[1 + K_y^2\right] \varepsilon(k)$$

$$\vdots$$

$$G_{2n+4} = -\frac{(2n+1)}{(2n+3)} K_y^2 G_{2n} + \frac{(2n+2)}{(2n+3)}[1 + K_y^2]G_{2n+2}$$

$$G_{2n+5} = -\frac{(n+1)}{(n+2)} K_y^2 G_{2n+1} + \frac{1}{2}\frac{(2n+3)}{(n+2)}[1 + K_y^2]G_{2n+3}$$

$$k^2 = 1 - K_y^2$$

$\kappa(k)$ = complete elliptic integral of the first kind

$\varepsilon(k)$ = complete elliptic integral of the second kind

If the above equations are derived in terms of the two Weibull parameters, m and σ_o, for shear sensitive cracks, then the critical crack strength parameter, M, becomes

$$M = \frac{\pi}{B\left(\frac{m+1}{2}, \frac{1}{2}\right)} \left(\frac{\sigma_x}{\sigma_o}\right)^m K_c^m$$

The parameters, m and c, are determined from the equations describing *Weibull fracture theory, and the parameter,* σ_o, *is determined from the* following expressions:

$$\sigma_o = \exp\left\{\frac{1}{m}\left[\ln A - C\right]\right\} \qquad \text{(uniaxial, pure tension)}$$

$$\sigma_o = \exp\left\{\frac{1}{m}\left[\ln\left(LW + \frac{LH}{m+1}\right) - C\right]\right\} \qquad \text{(uniaxial, pure bending)}$$

$$\sigma_o = \exp\left\{\frac{1}{m}\left[\ln A - \ln\frac{B\left(\frac{m+1}{2}, \frac{1}{2}\right)}{\pi} - C\right]\right\} \qquad \text{(equibiaxial, pure bending)}$$

The probability of survival for these cases then becomes,

$$\ln P_s = -A\left(\frac{\sigma}{\sigma_o}\right)^m \qquad \text{(uniaxial, pure tension)}$$

$$\ln P_s = -\left[LW + \frac{LH}{m+1}\right]\left(\frac{\sigma}{\sigma_o}\right)^m \qquad \text{(uniaxial, pure bending)}$$

$$\ln P_s = -\frac{\pi A}{B\left(\frac{m+1}{2}, \frac{1}{2}\right)}\left(\frac{\sigma}{\sigma_o}\right)^m \qquad \text{(equibiaxial, pure bending)}$$

and the probability of survival for a surface element in a biaxial stress state is found by numerical integration of the expression,

$$\ln P_s = - \frac{\pi \Delta A}{B\left(\frac{m+1}{2}, \frac{1}{2}\right)} \left(\frac{\sigma_x}{\sigma_o}\right)^m K_y^m - \Delta A \int_{K_y}^{1} \frac{2m}{B\left(\frac{m+1}{2}, \frac{1}{2}\right)} \left(\frac{\sigma_x}{\sigma_o}\right)^m \frac{K^{m-1}}{\sqrt{1 - K^2}} dK$$

where ω/π is evaluated for the stress state existing within the surface area element. The probability of dome survival is then determined by the method previously described.

This simplified method reduces to Weibull's method for uniaxial stress states and retains the effects of crack orientation in biaxial stress states. Values for the parameters, m and σ_o, for equibiaxial fracture data are shown in Table 3.

RESULTS

The volume and surface distributed crack theories of both Weibull and Batdorf (simplified version) were applied to the thermal stress distributions in the full-scale, MgF_2 domes that were subjected to the simulated free flight. A comparison between the predicted and observed probability of dome fracture as a function of time after the simulated launch is shown in Figures 20 through 24. All of the domes retained their geometric shape throughout the simulated free flight, even after dome fracture. Note that two curves representing predicted probability of dome fracture appear in each figure. These two curves represent probability of dome fracture for the maximum and minimum thermal stress levels that were observed at a given time in the simulated free-flight test series.

DISCUSSION

Examination of the fracture statistics that are available for MgF_2 shows that (1) the surface scratches on the uniaxial flexural test specimens are much larger than on a dome, and (2) the temperature dependence of the flexural strength for the equibiaxial test specimens is not known. Consequently, one would expect that the combination of large surface scratches and the effects of test specimen temperature would result in higher than actual probabilities of dome fracture for the fracture statistics obtained from the uniaxial flexural tests. Since the flexural strength of MgF_2 decreases with temperature, use of fracture statistics derived from equibiaxial flexural tests at room

temperature will tend to underpredict the probability of dome fracture. The optimum fracture theory for MgF_2 domes should therefore overpredict the probability of dome fracture when based on the uniaxial fracture data, and underpredict the probability of dome fracture when based on the equibiaxial fracture data. It is evident from the results shown in Figures 20 through 24, that only the surface distributed crack theory of Batdorf satisfies this criterion.

CONCLUSIONS

1. Fracture statistics obtained from flexural tests of small MgF_2 specimens can be used to predict the probability of fracture of full-scale domes in an aerodynamic heating environment.

2. The surface distributed flaw theory of Batdorf provides an accurate means of predicting the probability of dome fracture for the material, MgF_2.

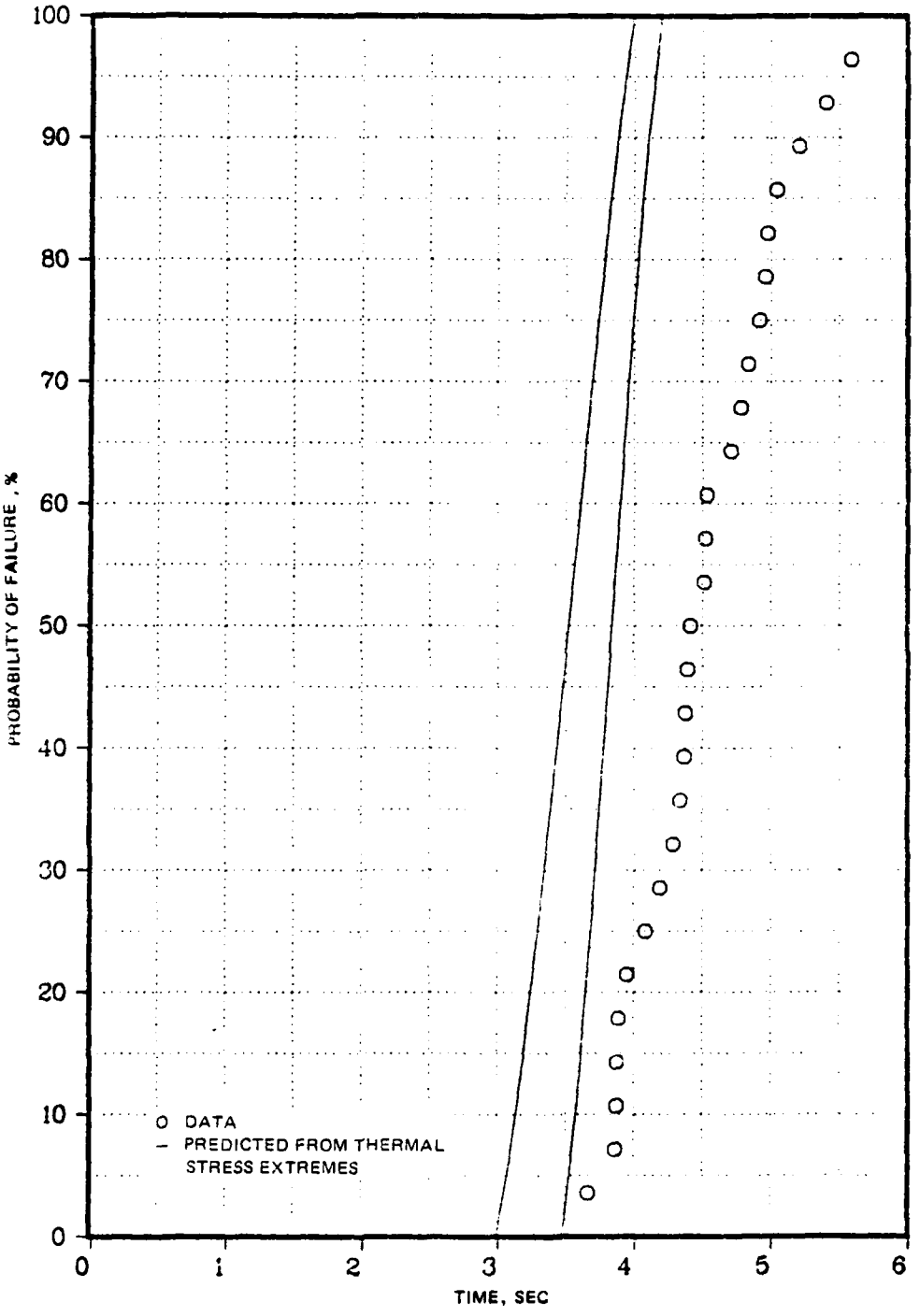

FIGURE 20. Comparison of Weibull Volume Theory and Dome Fracture Data (Uniaxial Fracture Statistics).

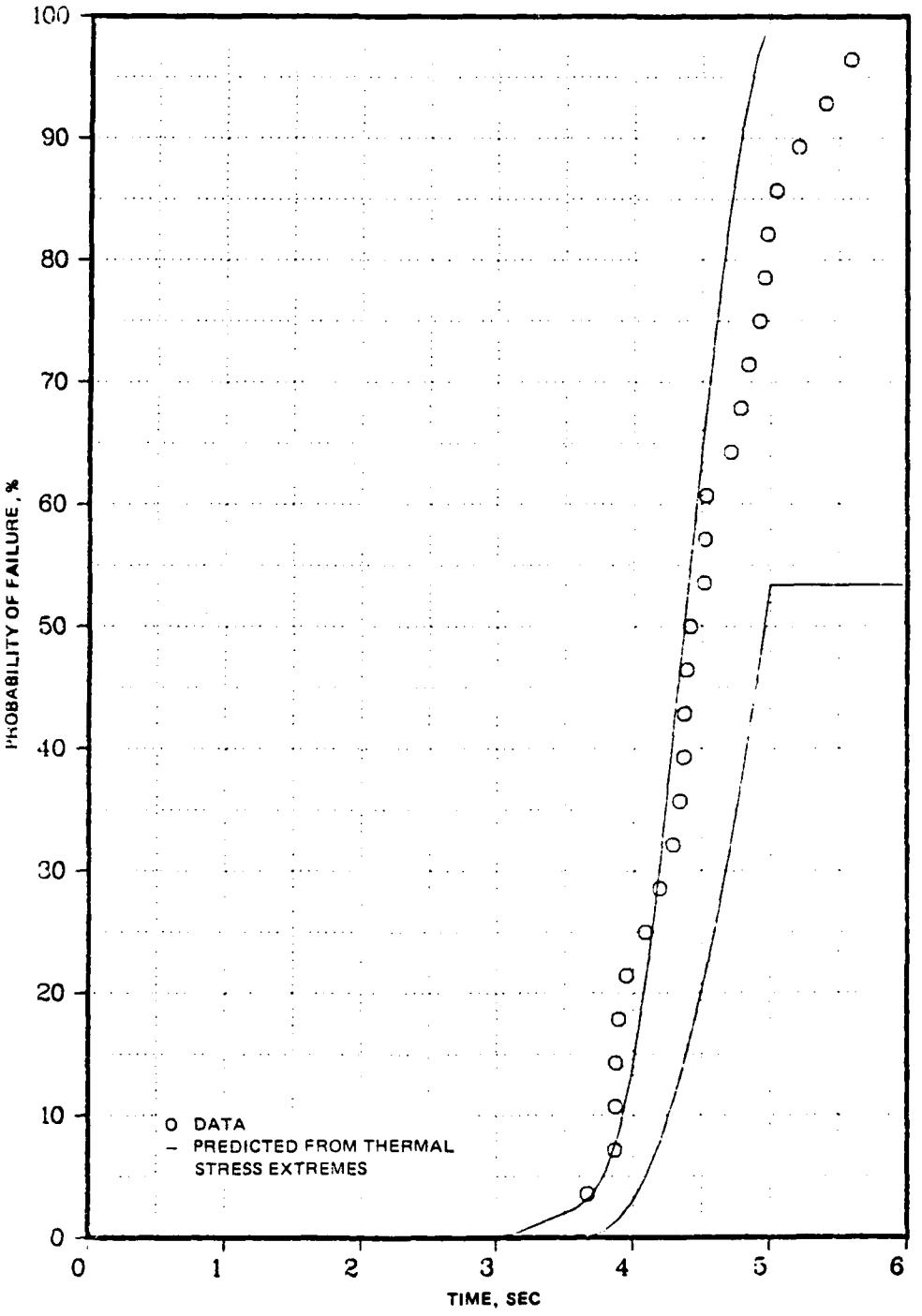

FIGURE 21. Comparison of Weibull Surface Theory and Dome Fracture Data (Uniaxial Fracture Statistics).

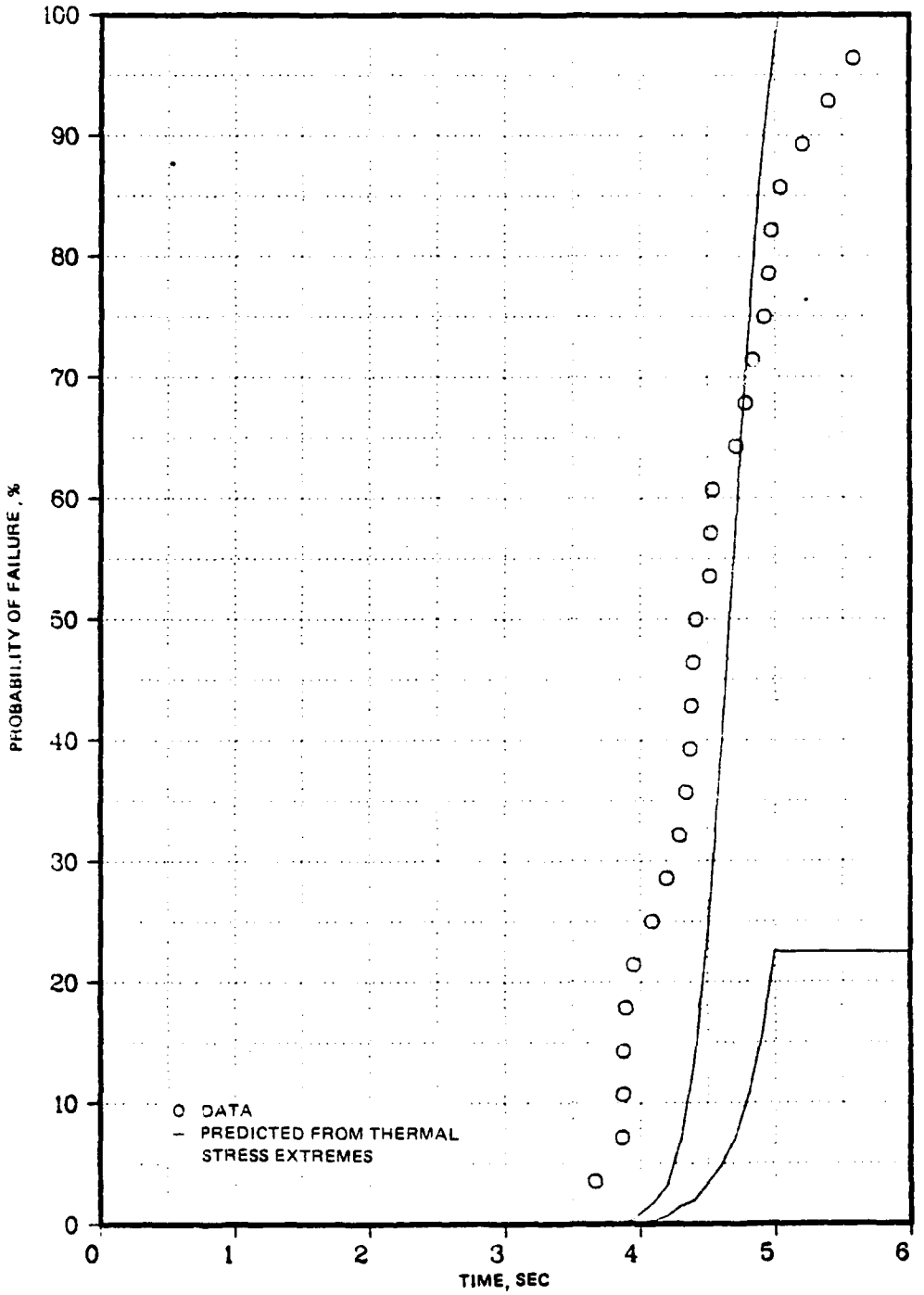

FIGURE 22. Comparison of Batdorf Volume Theory and Dome Fracture Data (Uniaxial Fracture Statistics).

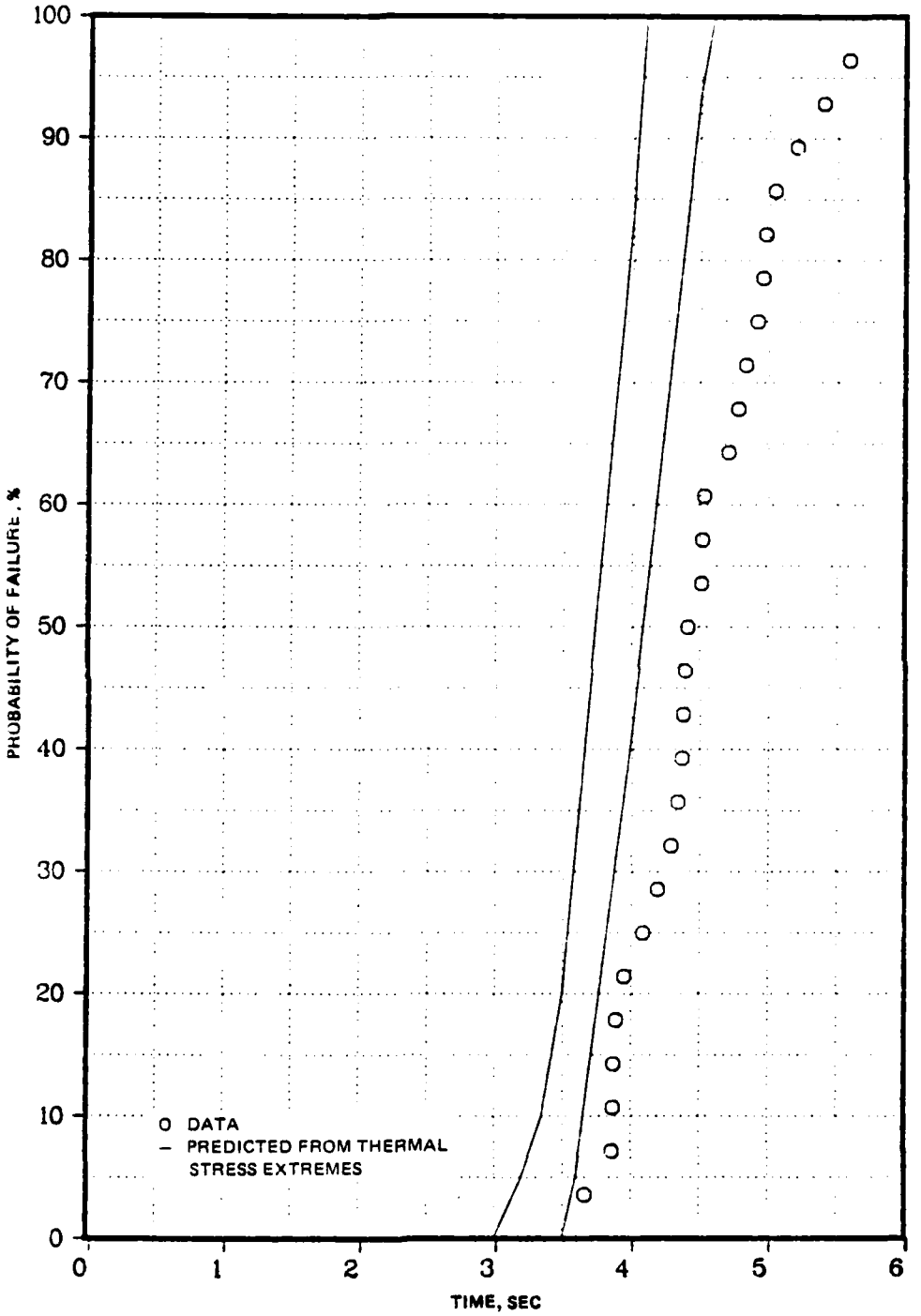

FIGURE 23. Comparison of Batdorf Surface Theory and Dome Fracture Data (Uniaxial Fracture Statistics).

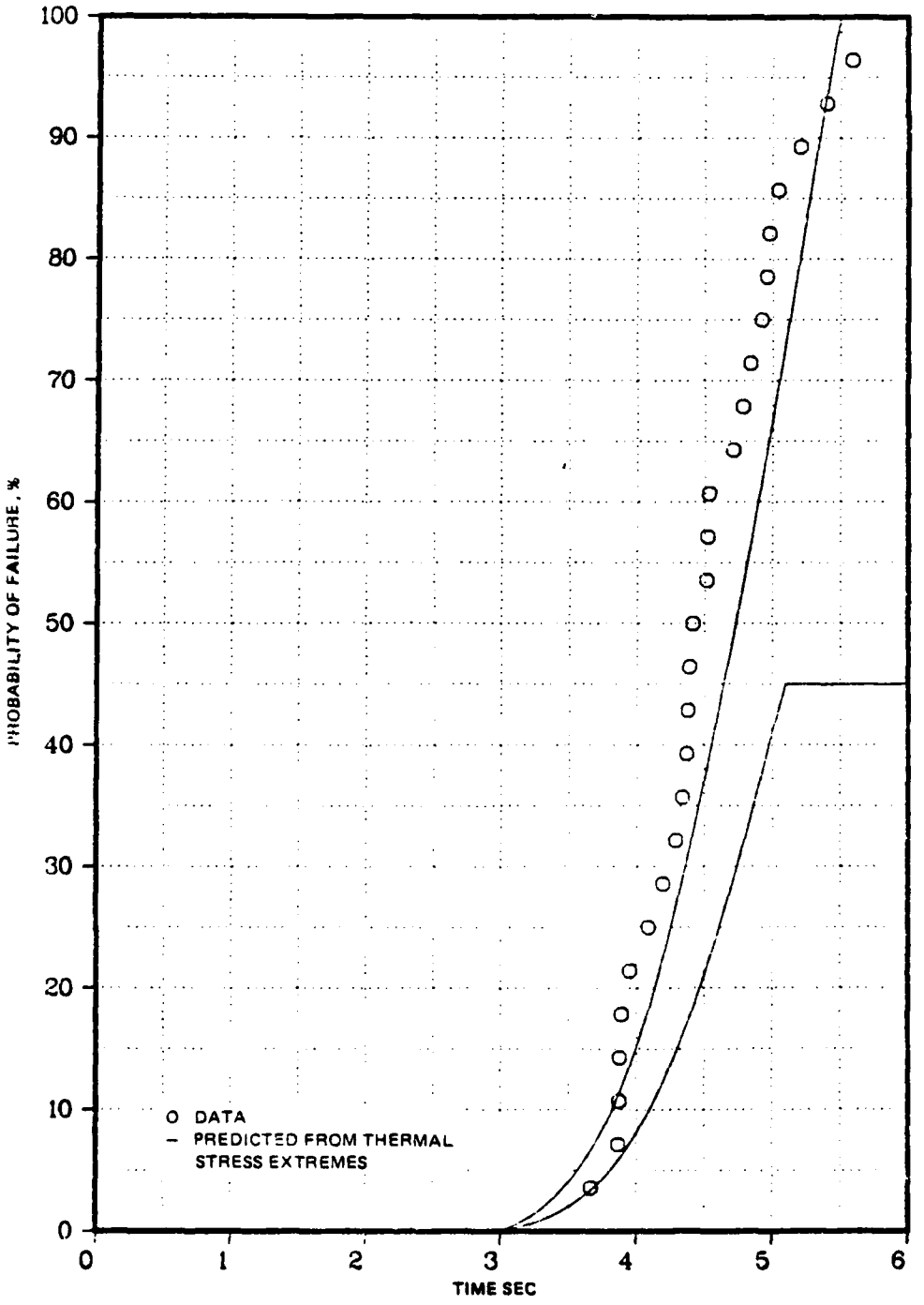

FIGURE 24. Comparison of Batdorf Surface Theory and Dome Fracture Data (Equibiaxial Fracture Statistics).

Appendix A

BATDORF VOLUME DISTRIBUTED FLAW THEORY

σ_x = principal stress in the x direction

σ_y = principal stress in the y direction

σ_z = principal stress in the z direction

σ_N = stress resulting from the principal stresses in direction normal to the plane of the crack

σ_n = component of σ_N in the $\sigma_y - \sigma_z$ plane

θ = angle between the σ_x axis and the crack normal

ϕ = angle between the σ_y axis and σ_n

Then for shear insensitive cracks,

$$\sigma_n = \sigma_y \cos^2\phi + \sigma_z \sin^2\phi$$

$$= \sigma_x[K_y - (K_y - K_z)\sin^2\phi]$$

$$\sigma_N = \sigma_x \cos^2\theta + \sigma_n \sin^2\theta$$

$$= \sigma_x \left\{[K_y - (K_y - K_z)\sin^2\phi] + [(1 - K_y) + (K_y - K_z)\sin^2\phi]\cos^2\theta\right\}$$

and for shear sensitive cracks

$$\sigma_n = \sigma_y \cos^2\phi + \sigma_z \sin^2\phi$$

$$= \sigma_x[K_y - (K_y - K_z)\sin^2\phi]$$

$$\sigma_N = \sigma_x \cos^2\theta + \sigma_n \sin^2\theta$$

$$= \sigma_x\left\{[K_y - (K_y - K_z)\sin^2\phi] + (1 - K_y) + (K_y - K_z)\sin^2\phi]\cos^2\theta\right\}$$

$$\tau_N = (\sigma_x - \sigma_n)\sin\vartheta\cos\vartheta$$

$$= \sigma_x[(1 - K_y) + (K_y - K_z)\sin^2\phi]\sin\vartheta\cos\vartheta$$

$$\sigma_{N_e}^2 = \sigma_N^2 + \tau_N^2$$

where

τ_N = shear in the crack plane

σ_{N_e} = effective stress normal to the crack plane

$K_y = \sigma_y/\sigma_x$

$K_z = \sigma_z/\sigma_x$

The limiting angle, θ_c, for which $\sigma_N \geq \sigma_c$ or $\sigma_{N_e} \geq \sigma_c$ is found by setting $\sigma_N = \sigma_c$, or $\sigma_{N_e} = \sigma_c$

$$\cos^2\vartheta_c = \frac{K_c - [K_y - (K_y - K_z)\sin^2\phi]}{1 - [K_y - (K_y - K_z)\sin^2\phi]} \quad \text{(shear insensitive)}$$

$$\cos^2\vartheta_c = \frac{K_c^2 - [K_y - (K_y - K_z)\sin^2\phi]^2}{1 - [K_y - (K_y - K_z)\sin^2\phi]^2} \quad \text{(shear sensitive)}$$

where

$K_c = \sigma_c/\sigma_x$

The solid angle over the stress ellipsoid for which $\sigma_N \geq \sigma_c$ or $\sigma_{N_e} \geq \sigma_c$ is then determined from the expression,

$$\Omega = 8\int_0^{\frac{\pi}{2}} d\phi \int_0^{\vartheta_c} \sin\theta\, d\theta = 4\pi - 8\int_0^{\frac{\pi}{2}} \cos\theta_c\, d\phi$$

or

$$\frac{\Omega}{4\pi} = 1 - \frac{2}{\pi}\int_0^{\frac{\pi}{2}} \cos\vartheta_c\, d\phi$$

The following special cases have been worked out for both the shear insensitive and shear sensitive cases:

Shear Insensitive Cracks

$$\frac{\Omega}{4\pi} = 1 - \sqrt{K_c} \qquad (K_y = K_z = 0) \qquad \text{(uniaxial)}$$

$$\frac{\Omega}{4\pi} = \sqrt{1 - K_c} \qquad (K_y = 1,\ K_z = 0) \qquad \text{(equibiaxial)}$$

Shear Sensitive Cracks

$$\frac{\Omega}{4\pi} = 1 - K_c \qquad (K_y = K_z = 0) \qquad \text{(uniaxial)}$$

$$\frac{\Omega}{4\pi} = \sqrt{1 - K_c^2} \qquad (K_y = 1,\ K_z = 0) \qquad \text{(equibiaxial)}$$

Expressions for the quantity, $\Omega/4\pi$, have currently been derived only for shear insensitive cracks in a general triaxial stress state. The expressions derived for shear insensitive cracks are as follows:

$(K_y \geq K_c \geq 1)$

$$\frac{\Omega}{4\pi} = 1 - A_o(\beta, k)$$

$$\beta = \sin^{-1}\sqrt{\frac{K_c - K_z}{1 - K_z}}$$

$$k = \sqrt{\frac{(1 - K_c)(K_y - K_z)}{(1 - K_y)(K_c - K_z)}}$$

$(K_z \leq K_c \leq K_y)$

$$\frac{\Omega}{4\pi} = A_o(\beta, k)$$

$$\beta = \sin^{-1}\sqrt{\frac{1 - K_c}{1 - K_z}}$$

$$k = \sqrt{\frac{(1 - K_y)(K_c - K_z)}{(1 - K_c)(K_y - K_z)}}$$

$(0 \leq K_c \leq K_z)$

$$\frac{\Omega}{4\pi} = 1$$

where

$\Lambda_o(\beta,k)$ is Heuman's Lambda function

Using the approximation,

$$\Lambda_o(\beta,k) = (1 - k^2)\sin\beta + \frac{2}{\pi} k^2 \beta$$

the above expressions for $\Omega/4\pi$ become,

$(K_y \leq K_c \leq 1)$

$$\frac{\Omega}{4\pi} \cong 1 - 1\left[- \frac{(1 - K_c)(K_y - K_z)}{(1 - K_y)(K_c - K_z)}\right]\sqrt{\frac{K_c - K_z}{1 - K_z}}$$

$$- \frac{2}{\pi} \frac{(1 - K_c)(K_y - K_z)}{(1 - K_y)(K_c - K_z)} \sin^{-1}\sqrt{\frac{K_c - K_z}{1 - K_z}}$$

$(K_z \leq K_c \leq K_y)$

$$\frac{\Omega}{4\pi} \cong \left[1 - \frac{(1 - K_y)(K_c - K_z)}{(1 - K_c)(K_y - K_z)}\right]\sqrt{\frac{1 - K_c}{1 - K_z}}$$

$$+ \frac{2}{\pi} \frac{(1 - K_y)(K_c - K_z)}{(1 - K_c)(K_y - K_z)} \sin^{-1}\sqrt{\frac{1 - K_c}{1 - K_z}}$$

$(0 \leq K_c \leq K_z)$

$$\frac{\Omega}{4\pi} = 1$$

which can be readily reduced to the results obtained for the special cases of uniaxial and equibiaxial stress states. The corresponding expressions for shear sensitive cracks involve rather messy hyperelliptic integrals and are probably best treated via numerical integration techniques.

If the critical crack strength parameter, N, is expressed in the form,

$$N = \sum_{n=1} a_n \sigma_c^n = \sum_{n=1} a_n \sigma_x^n K_c^n$$

Then the following expressions can be developed from the special case relations for $\Omega/4\pi$:

Shear Insensitive Cracks

$$\ell n P_s = - V \sum_{n=1} \frac{a_n \sigma_m^n}{(2n + 1)} \qquad \text{(uniaxial, pure tension)}$$

$$\ell n P_s = - \frac{V}{2} \sum_{n=1} \frac{a_n \sigma_m^n}{(n + 1)(2n + 1)} \qquad \text{(uniaxial, pure bending)}$$

$$\ell n P_s = - \frac{V}{2} \sum_{n=1} \frac{n}{(n + 1)} a_n \sigma_m^n B\left(n, \frac{3}{2}\right) \qquad \text{(equibiaxial, pure bending)}$$

Shear Sensitive Cracks

$$\ell n P_s = - V \sum_{n=1} \frac{a_n \sigma_m^n}{(n + 1)} \qquad \text{(uniaxial, pure tension)}$$

$$\ell n P_s = - \frac{V}{2} \sum_{n=1} \frac{a_n \sigma_m^n}{(n + 1)^2} \qquad \text{(uniaxial, pure bending)}$$

$$\ell n P_s = - \frac{V}{4} \sum_{n=1} \frac{n}{(n + 1)} a_n \sigma_m^n B\left(\frac{n}{2}, \frac{3}{2}\right) \qquad \text{(equibiaxial, pure bending)}$$

where

σ_m = maximum tensile stress

B = Beta function

The coefficients, a_n, in the series above can be determined from material specimens by fitting a least-squares polynomial to the fracture data.

$$\ell nP_s - \ell_n \left[\frac{N + 1 - n}{N + 1}\right] = -\sum_{i=1} b_i \sigma_m^i$$

where

N = total number of specimens tested

n = number of specimens that failed at a maximum tensile stress, σ_m, or lower

b_i = least-squares polynomial coefficients for fracture data

If the four-point bending tests have been used, for example, then the a_n coefficients can be expressed in terms of the b_n coefficients of the least-squares fit to the fracture data.

$$a_n = 2(n + 1)(2n + 2)\frac{b_n}{V} \qquad \text{(uniaxial, shear insensitive)}$$

$$a_n = 2(n + 1)^2 \frac{b_n}{V} \qquad \text{(uniaxial, shear sensitive)}$$

The probability of survival of a material volume element is then expressed as

$$\ell nP_s = -\int dV \int_0^1 \frac{\Omega}{4\pi} \sum_{n=1} n a_n \sigma_x^n K_c^{n-1} dK_c$$

for triaxial stress states. The maximum principal stress, σ_x, can be determined from a finite-element stress analysis of the geometry in question and the a_n coefficients are determined from fracture test data obtained in a more convenient stress state (e.g., uniaxial). The probability of survival for the geometry in question is then equal to the product of the survival probabilities for the individual volume elements in the finite-element model.

Appendix B

BATDORF SURFACE DISTRIBUTED FLAW THEORY

If θ = constant = 0, in the expression for θ_c (Appendix A), then

$$\sin \theta_c = \sqrt{\frac{1 - K_c}{1 - K_y}} \qquad \text{(shear insensitive)}$$

$$\sin \theta_c = \sqrt{\frac{1 - K_c^2}{1 - K_y^2}} \qquad \text{(shear sensitive)}$$

and for $\omega = 2\theta_c$

$$\frac{\omega}{\pi} = \frac{2}{\pi} \sin^{-1} \sqrt{\frac{1 - K_c}{1 - K_y}} \qquad \text{(shear insensitive)}$$

$$\frac{\omega}{\pi} = \frac{2}{\pi} \sin^{-1} \sqrt{\frac{1 - K_c^2}{1 - K_y^2}} \qquad \text{(shear sensitive)}$$

The probability of survival of an element of surface area is given by

$$\ln P_s = -\int dA \int \frac{\omega}{\pi} \frac{dM}{d\sigma_c} d\sigma_c = \int dA \int M d\left(\frac{\omega}{\pi}\right)$$

or

$$-\ln P_s = \int \frac{dA}{\pi} \int_{K_y}^{1} \frac{dK_c}{\sqrt{1 - K_c}\sqrt{K_c - K_y}} \qquad \text{(shear insensitive)}$$

$$-\ln P_s = \int \frac{2dA}{\pi} \int_{K_y}^{1} \frac{K_c dK_c}{\sqrt{1 - K_c^2}\sqrt{K_c^2 - K_y^2}} \qquad \text{(shear sensitive)}$$

If the critical strength parameter, M, is expressed as the series

$$M = \sum_{n=1} a_n \sigma_x^n K_c^n$$

then

$$-\ln P_s = \int \frac{1}{\pi} \sum_{n=1} a_n \sigma_x^n \int_{K_y}^{1} \frac{K_c^n dK_c}{\sqrt{1 - K_c}\sqrt{K_c - K_y}} dA \qquad \text{(shear insensitive)}$$

$$-\ln P_s = \int \frac{2}{\pi} \sum_{n=1} a_n \sigma_x^n \int_{K_y}^{1} \frac{K_c^{n+1} dK_c}{\sqrt{1 - K_c^2}\sqrt{K_c^2 - K_y^2}} dA \qquad \text{(shear sensitive)}$$

The integral for the shear insensitive case is of the form,

$$I_n = \int_{K_y}^{1} \frac{x^n dx}{\sqrt{Y}},$$

where

$$Y = a + bx + cx^2$$

and

$$a = -K_y, \; b = (1 + K_y), \; c = -1$$

Evaluating these integrals,

$$I_o = \frac{1}{\sqrt{-c}} \left[\sin^{-1} \left(\sqrt{\frac{-2cx - b}{b^2 - 4ac}} \right) \right]_{K_y}^{1}$$

$$I_1 = -\frac{b}{2c} I_o$$

$$I_2 = \frac{(3b^2 - 4ac)}{8c^2} I_o$$

$$I_3 = \left[\frac{3ab}{4c^2} - \frac{5b^3}{16c^3} \right] I_o$$

and

$$I_n = -\frac{(2n-1)}{n}\frac{b}{2c} I_{n-1} - \frac{(n-1)}{n}\frac{a}{c} I_{n-2}$$

Therefore,

$$-\delta nP_s = \int \frac{1}{\pi} \sum_{n=1} a_n \sigma_x^n I_n dA \qquad \text{(shear insensitive)}$$

The corresponding integral for the shear sensitive case reduces to the form

$$G_{n+1} = G_m = \int_o^{\frac{\pi}{2}} \left[1 - k^2 \sin^2 x\right]^{\frac{(m-1)}{2}} dx$$

where

$$x = \sin^{-1}\sqrt{\frac{1-t^2}{1-K_y^2}}$$

$$k^2 = 1 - K_y^2$$

$$t = K_c^2$$

Evaluating these integrals

$$G_o = \kappa(\kappa)$$

$$G_1 = \frac{\pi}{2}$$

$$G_2 = \varepsilon(k)$$

$$G_3 = \frac{\pi}{4}(1 + K_y^2)$$

$$G_4 = -\frac{1}{3} K_y^2 \kappa(k) + \frac{2}{3}(1 + K_y^2)\varepsilon(k)$$

and

$$G_{2n+4} = -\frac{(2n+1)}{(2n+3)} K_y^2 G_{2n} + \frac{(2n+2)}{(2n+3)}(1 + K_y^2) G_{2n+2}$$

$$G_{2n+5} = -\frac{(n+1)}{(n+2)} K_y^2 G_{2n+1} + \frac{1}{2}\frac{(2n+3)}{(n+2)}(1 + K_y^2) G_{2n+3}$$

Therefore

$$-\delta nP_s = \int \frac{2}{\pi} \sum_{n=1} a_n \sigma_x^n G_{n+1} dA \qquad \text{(shear sensitive)}$$

INITIAL DISTRIBUTION

13 Naval Air Systems Command
- AIR-03A (1)
- AIR-03E (1)
- AIR-03P2 (1)
- AIR-30212 (2)
- AIR-320 (1)
- AIR-320B (1)
- AIR-320C (1)
- AIR-5108 (1)
- AIR-5323 (1)
- AIR-53242 (1)
- AIR-950D (2)

1 Chief of Naval Operations

6 Naval Sea Systems Command
- SEA-033 (1)
- SEA-03513 (1)
- SEA-62R41 (1)
- SEA-6543 (1)
- SEA-99612 (2)

1 Chief of Naval Research, Arlington (ONR-461)

3 David Taylor Naval Ship Research and Development Center, Bethesda
- Code 1606 (1)
- Code 166 (1)
- Code 167 (1)

2 Naval Air Development Center, Johnsville, Warminster
- Code 01A (1)
- Technical Library (1)

1 Naval Air Engineering Center, Lakehurst

1 Naval Air Test Center (CT-176), Patuxent River (Aeronautical Publications Library)

1 Naval Avionics Center, Indianapolis (Technical Library)

1 Naval Ocean Systems Center, San Diego (Code 1311)

1 Naval Ordnance Station, Indian Head

1 Naval Postgraduate School, Monterey

2 Naval Research Laboratory
- Code 2021 (1)
- Code 6360, R. W. Rice (1)

9 Naval Surface Weapons Center Detachment, White Oak Laboratory, Silver Spring
- G-41 (1)
- K-04 (1)
- K-21 (1)
- K-80 (1)
- K-81 (1)
- K-82 (1)
- R-44 (1)
- Technical Library (2)

1 Operational Test & Evaluation Force, Norfolk
3 Pacific Missile Test Center, Point Mugu
  Code 0101 (1)
  Code 3132 (1)
  Technical Library (1)
3 U.S. Army Missile Command, Redstone Scientific Information Center, Redstone Arsenal (DRSMI-RPRD)
4 Aberdeen Proving Ground
  Dr. B. Karpov (2)
  Development and Proof Services (2)
2 Army Ballistic Research Laboratories, Aberdeen Proving Ground
  DRDAR-TSB-S (STINFO) (1)
1 Tactical Air Command, Langley Air Force Base (TPL-RQD-M)
1 Air University Library, Maxwell Air Force Base
2 Armament Development & Test Center, Eglin Air Force Base
  AFATL/ADLA (1)
  Directorate of Ballistics, A. S. Galbraith (1)
12 Defense Technical Information Center
1 Weapons Systems Evaluation Group
1 Lewis Research Center, NASA, Cleveland
1 Applied Physics Laboratory, JHU, Laurel, MD (Document Library)
1 Ceradyne, Inc., Santa Ana, CA (J. Rubin)
1 Chemical Propulsion Information Agency, APL, Laurel, MD
1 Coors Porcelain Co., Golden, CO (D. Roy)
1 Jet Propulsion Laboratory, CIT, Pasadena, CA (Technical Library)
1 Massachusetts Institute of Technology, Aerophysics Laboratory, Cambridge, MA
1 The Rand Corporation, Santa Monica, CA (Aero-Astronautics Dept.)


DA
FILM